

COMPARISON OF DAMPING ON VARIOUS JOINTED STRUCTURES

A THESIS SUBMITTED IN PARTIAL FULFILLMENT
OF THE REQUIREMENTS FOR THE DEGREE OF

MASTER OF TECHNOLOGY
IN
MECHANICAL ENGINEERING

BY

PRANEETH KUMAR BALASANKULA
210ME2239



DEPARTMENT OF MECHANICAL ENGINEERING
NATIONAL INSTITUTE OF TECHNOLOGY
ROURKELA
2012

COMPARISON OF DAMPING ON VARIOUS JOINTED STRUCTURES

A THESIS SUBMITTED IN PARTIAL FULFILLMENT
OF THE REQUIREMENTS FOR THE DEGREE OF

MASTER OF TECHNOLOGY
IN
MECHANICAL ENGINEERING

BY

PRANEETH KUMAR BALASANKULA
210ME2239

UNDER THE GUIDANCE OF

Prof. B.K. NANDA



**DEPARTMENT OF MECHANICAL ENGINEERING
NATIONAL INSTITUTE OF TECHNOLOGY
ROURKELA
2012**



**National Institute of Technology
Rourkela**

CERTIFICATE

This is to certify that the thesis entitled, “**COMPARISON OF DAMPING ON VARIOUS JOINTED STRUCTURES**” submitted by Mr. Praneeth kumar balasankula in partial fulfillment of the requirements for the award of *Master of Technology* degree in *Mechanical Engineering* with specialization in *Production Engineering* during session 2010-2012 at the National Institute of Technology, Rourkela.

It is an authentic work carried out by him under my supervision and guidance. To the best of my knowledge, the matter embodied in the thesis has not submitted to any other University/Institute for the award of any degree or diploma.

Date:

Place:

Prof. B.K. Nanda
Dept. of Mechanical Engg.
National Institute of Technology

ACKNOWLEDGEMENT

Successful completion of work will never be one man's task. It requires hard work in right direction. There are many who have helped to make my experience as a student a rewarding one. In particular, I express my gratitude and deep regards to my thesis supervisor **Dr. B.K. Nanda, Professor, Department of Mechanical Engineering, NIT Rourkela** for kindly providing me to work under his supervision and guidance. I extend my deep sense of indebtedness and gratitude to him first for his valuable guidance, inspiring discussions, constant encouragement & kind co-operation throughout period of work which has been instrumental in the success of thesis.

I extend my thanks to **Dr. K.P. Maity, Professor and Head, Dept. of Mechanical Engineering, Department of Mechanical Engineering, NIT Rourkela** for extending all possible help in carrying out the dissertation work directly or indirectly.

I greatly appreciate and convey my heartfelt thanks to my friends Piyush swamy, Elias Eliot, D. Sahitya , Arundathi Pradhan ,Hemanth Rana , Ashirbad Swain , dear ones & all those who helped me in completion of this work.

I feel pleased and privileged to fulfill my parent's ambition and I am greatly indebted to them for their moral support and continuous encouragement while carrying out this study. This thesis is dedicated to my family.

PRANEETH KUMAR BALASANKULA

Abstract

Light weight structures commonly have low connate structural damping. The damping mechanism of various jointed structures can be explained by considering the energy loss due to friction and the dynamic slip produced at the interfaces. The frictional damping is evaluated from the relative slip between the jointed interfaces and is considered to be the most useful method for inspect the structural damping. The damping characteristics in jointed structures are influenced by the intensity of pressure distribution, micro-slip kinematic coefficient of friction and logarithmic decrement at the interfaces. The effects of all these parameters on the mechanism of damping have been extensively studied. All the above basic parameters are largely influenced by the thickness ratio of the beam and thereby affect the damping capacity of the structures. In addition to this, beam length of the structures and diameter of connecting rivet and bolt also play key roles on the damping capacity of the jointed structures is assessable. For rivet bolt & welded joints the theoretical analysis proposes two different methods to calculate damping: classical method and finite element method. The analyses are based on the assumptions of Euler-Bernoulli beam theory as the dimensions of test specimens satisfy the criterion of thin beam theory. The effects of all these parameters are studied distinctly in the present investigation. It is established that the damping capacity can be increased appreciably using larger beam length and their diameters as well as lower thickness ratio of the beams. This design concept of using these structures can be effectively utilized in trusses and frames, aircraft and aerospace structures, bridges, machine members, robots and many other applications where higher damping is required. Comprehensive experiments have been conducted on a number of mild steel specimens under different initial conditions of excitation for establishing the accuracy of the theory developed. Finally damping on various joint structures has been compared.

Contents

Certificate.....	iii
Acknowledgement	iv
Abstract.....	v
List Of Tables.....	ix
Nomenclature.....	x
<i>1 INTRODUCTION</i>	1
1.1 Damping.....	3
1.2 Classification of Damping	4
1.2.1 Structural Damping at Joints and Interfaces	4
1.3 Measurement of Structural Damping.....	5
1.3.1 Logarithmic Decrement (δ).....	5
1.3.2 Quality Factor (Q).....	6
1.3.3 Damping Ratio (ζ).....	8
1.3.4 Specific Damping Capacity (Ψ).....	9
1.3.5 Loss Factor (η).....	9
1.4 Linear Problem.....	10
1.5 Beam Theories	11
1.6 Modeling of a Structure	12
1.6.1 Classification of Joints According To Configuration	13
1.6.2 Damping Due To Sandwich Construction	14
1.7 Different Techniques of Damping	14
1.8 Various Types of Jointed Structures	17
1.9 Aims and Objectives	19
<i>2 LITERATURE SURVEY</i>	20
<i>3 THEORETICAL ANALYSIS</i>	26
3.1 Interface Pressure Distribution.....	27
3.1.1 Determination of Pressure Distribution at the Interfaces for Riveted and Bolted Joints	28
3.2 Dynamic Equations of Free Transverse Vibration of Fixed-Fixed Beams.	30

3.2.1	Introduction.....	30
3.3	Dynamic equations for free transverse vibration on various joint structures.....	30
3.3.1	Evaluation of Constants A1, A2, A3 and A4	33
3.3.2	Evaluation of constants A5 and A6	34
3.3.3	Evaluation of relative dynamic slip	36
3.3.5	Evaluation Of Damping Ratio.....	39
3.3.6	Logarithmic decrement	39
4	<i>EXPERIMENTATION</i>	41
4.1	Experimental Set-Up.....	42
4.2	Instrumentation	47
4.3	Connecting an oscilloscope.....	50
4.4	Voltage	52
4.5	Time period.....	52
4.6	Dial indicator	52
4.7	Vibration pick-up	53
4.8	Theory of Operation.....	54
4.8.1	Signal Conventions	55
4.8.2	Construction	55
4.9	Experimental Techniques.....	56
5	<i>RESULTS AND DISCUSSION</i>	58
5.1	Results for coefficient of friction $\mu * \alpha$ versus frequency	59
5.2	Results for variation of logarithmic decrement with length of specimen for fixed-fixed beams.....	61
5.3	Result for variation of logarithmic decrement with amplitude of excitation for fixed-fixed beam by varying length	62
5.4	Result for variation of logarithmic decrement with torque for fixed-fixed beam:	63
5.5	Result for variation of logarithmic decrement with diameter of rivet and bolt joints.....	63
6	<i>CONCLUSIONS AND SCOPE FOR FURTHER WORK</i>	65
	<i>REFERENCES</i>	68

List of Figures

Figure.1 Q-factor method of damping measurement	7
Figure 2 Free vibration of systems with different levels of damping.	9
Figure 3 Comparison of Linear and nonlinear systems	11
Figure 4 Free body diagram of bolted joint showing influence zone.....	28
Figure 5 variation of damping in a fixed-fixed beam	32
Figure 6 Details of mild steel specimens used in the experiment for the thickness ratio 1.0 for riveted, bolted and welded joints	43
Figure 7 Schematic diagram of riveted joint in fixed-fixed beam	44
Figure 8 Schematic diagram of welded joint in fixed-fixed beam.....	45
Figure 9 Schematic diagram of bolted joint in fixed-fixed beam	45
Figure 10 storage oscilloscope.....	49
Figure 11 nodes showing voltage vs time	51
Figure 12 dial gauge.....	53
Figure 13 vibration pickup	54
Figure 14 deflection for fixed-fixed beam.....	59
Figure 15 Variation of α, μ with frequency of vibration for mild steel specimens with beam for rivet joint	59
Figure 16 Variation of α, μ with frequency of vibration for mild steel specimens with beam for bolted joint	60
Figure 17 Variation of α, μ with frequency of vibration for mild steel specimens with beam for welded joint	60
Figure 18 Variation of logarithmic decrement with the length of specimen of mild steel with amplitude of excitation 0.1 mm.	61
Figure 19 Variation of logarithmic decrement with the length using mild steel with amplitude of excitation 0.2 mm.....	61
Figure 20 Variation of logarithmic decrement with the length using mild steel with amplitude of excitation 0.3 mm.....	62
Figure 21 Variation of logarithmic decrement with initial amplitude of excitation	62
Figure 22 Variation of logarithmic decrement with applied tightening torque.....	63
Figure 23 Variation of logarithmic decrement with diameter of rivet of 1.0 thickness ratio.....	63
Figure 24 Variation of logarithmic decrement with diameter of bolt of 1.0 thickness ratio.....	64

List Of Tables

Table 1	Details of mild steel specimens used in the experiment for the thickness ratio 1.0 in riveted joints.....	46
Table 2	Details of mild steel specimens used in the experiment for the thickness ratio 1.0 in bolted joints	46
Table 3	Details of mild steel specimens used in the experiment for the thickness ratio 1.0 in welded joints.....	47

Nomenclature

English Symbols

A	Area of cross-section of the beam
A_o	Area of cross-section of the rivet
A'	Area under a connecting rivet head
d	Diameter of connecting rivet
E	Static bending modulus of elasticity
E_f	Energy loss per cycle due to friction at joints
E Loss	E Total energy loss per cycle
E_n	Energy stored in the system per cycle
E	Energy loss per cycle due to material and support friction
RMF	Maximum frictional force at the interfaces
I	Second moment of area
K	Static bending stiffness of the layered and jointed beam
K'	Static bending stiffness of the solid beam
l	Length of individual elements
L	Free length of the layered and jointed beam
M	Number of layers in a jointed beam
N	Total normal force under each connecting rivet
p	Interface pressure
P	Preload on a rivet
q	Number of rivets

R	Any radius within influencing zone
R_B	Radius of the connecting rivet
R_M	Limiting radius of influencing zone
t	time coordinate
U_o friction	Relative dynamic slip between the interfaces at a riveted joint in the absence of friction
U_r friction	Relative dynamic slip between the interfaces at a riveted joint in the presence of friction
U_{rm} vibration	Relative dynamic slip between the interfaces at the maximum amplitude of vibration
W	Static load
a_1, a_{n+1}	Amplitude of first cycle and last cycle, respectively
$y(l, 0)$	Initial free end displacement
n	Number of cycles

Greek Symbols

α	Dynamic slip ratio (α)
δ	Logarithmic decrement of the system
Δ	Deflection due to static load
μ	Kinematic coefficient of friction
ω_n	Natural frequency of vibration
ω_d	Damped frequency of vibration
ρ	Mass density
σ_0	Initial stress on a rivet
σ_s	Surface stress on the jointed structure
ξ	Damping ratio

CHAPTER – 1

INTRODUCTION

With accelerated growth and development of disenchanted contrive structures, efforts have been made by engineers and technologists to improve their capabilities by checking disastrous effects of vibration transmitted through foundation and chatter of fabricated structures. Problems involving vibration occur in many areas of mechanical, civil and aerospace engineering. Engineering structures are generally fabricated using a variety of connections such as bolted, riveted, welded and bonded joints etc. The dynamics of mechanical joints is a topic of special interest due to their strong influence in the performance of the structure. Further, the inclusion of these joints plays a significant role in the overall system behavior, particularly the damping level of the structures. However, the determination of damping either by analysis or experiment is never straightforward owing to the complexity of the dynamic interaction of components. The estimation of damping in beam-like structures with passive damping approach is the essential problem addressed by the present research. The study of dynamics of fabricated structures, a subject of comparatively of recent origin, enables us to design machines which could minimize the machining error that are liable to creep into the job under the dynamic condition, viz. deflection, positional error, error due to vibrational instability. The continuous trend towards lighter structure, low noise, increased reliability, highly balance, less vibration transmission to foundation and long life at higher operating speed requires that research work in this field will remain important in future. Friction damping takes place whenever two surfaces experience relative motion in the presence of friction. In case of a jointed structure, the relative motion between contacting layers is a function of normal load which arises from the tightening of the joints holding the components. When the joint is very loose, the normal load is insignificant and the contact surface experiences pure slip. Since no work is required to be done against friction, no energy is dissipated. On the other hand, when the joint is very tight, high

normal loads cause the whole contact interface to stick. This results in no energy dissipation again since no relative motion is allowed at the interfaces. For normal loads lying between these two extremities, energy is dissipated and the maximum value of energy dissipation occurs within this range. The contact pressure between the surfaces is generated by the clamping action of the joints and plays a vital role in the joint properties. Due to uneven pressure distribution, a local relative motion termed as micro-slip occurs at the interfaces of the connecting members. The energy dissipated in most real structures is often very small, so that an undamped analysis is sometimes realistic. When the damping is significant, its effect must be included in the analysis particularly when the dynamic study of a structure is required. The energy of the vibrating system is dissipated by various mechanisms and often more than one mechanism may be present at the same time. Although the knowledge on the friction joint is limited, efforts have been put in the present investigation to study the damping aspect of the friction joints in built-up structures.

1.1 Damping

Damping is the energy dissipation properties of a material or system under cyclic stress. When a structure is subjected to an excitation by an external force then it vibrates in certain amplitude of vibration, it reduces as the external force is removed. This is due to some resistance offered to the structural member which may be internal or external. This resistance is termed as damping. The origin and mechanism of damping are complex and sometimes difficult to comprehend. The energy of the vibrating system is dissipated by various mechanisms and often more than one mechanism may be present simultaneously. For convenience, damping is divided into two major groups identified as:

1.2 Classification of Damping

Damping can be broadly divided into two classes depending on their sources,

(1) Material damping

(2) System damping

Material Damping:

Material damping, also called solid or material damping, is related to the energy dissipation within the volume of material. This mechanism is usually associated with internal reconstructions of the micro and macro structure ranging from crystal lattice to molecular scale effects, thermo-elasticity, grain boundary viscosity, point-defect relaxation, etc. [1, 2]. Besides, there are two types of internal damping: hysteretic damping and visco-elastic damping.

System Damping:

System damping involves configuration of distinguishable part arises from slip and boundary shear effects of mating surfaces. Energy dissipation during cyclic stress at an interface may occur as a result of dry sliding (coulomb friction), lubricated sliding (viscous forces) or cyclic strain in a separating adhesive (damping in visco-elastic layers between mating surfaces).

1.2.1 Structural Damping at Joints and Interfaces

Since the damping in the structural material is not significant, most of the damping in real fabricated structures arises in the joints and interfaces [1]. It is the result of energy dissipation caused by rubbing friction resulting from relative motion between components and by intermittent contact at the joints in a mechanical system. However, the energy dissipation

mechanism in a joint is a complex phenomenon being largely influenced by the interface pressure and degree of slip at the interfaces. It is this slip phenomenon occurring in the presence of friction at the joint interface that causes the energy dissipation and nonlinearity in the joints.

1.3 Measurement of Structural Damping

There are several ways of expressing the damping in a structure. They are time response and frequency-response methods where the response of the system is expressed in terms of time and frequency, respectively. Depending on the mathematical model of the physical problem, the above two methods are used to measure the damping capacity of the structures. Logarithmic decrement (δ) is determined using time domain method and the quality factor(Q) by frequency domain method. However, the other nomenclatures such as; damping ratio(ζ), specific damping capacity(ψ) and loss factor(η) are estimated from either of the above two methods for measuring the damping.

1.3.1 Logarithmic Decrement (δ)

The logarithmic decrement method is the most widely used time-response method to measure damping from the free-decay of the time history curve. When the structure is set into free vibration, the fundamental mode dominates the response since all the higher modes are damped out quickly. The logarithmic decrement represents the rate at which the amplitude of a free damped vibration decreases. It is defined as the natural logarithm of the ratio of any two successive amplitudes. Thus, the logarithmic decrement δ is obtained as;

$$\delta = \frac{\ln(x_1)}{x_2} = \frac{2\pi\zeta}{\sqrt{1-\zeta^2}} \quad (1)$$

Where, x_1 and x_2 are the successive amplitudes and ζ is the damping ratio.

For small damping, the above relation is approximated as; $\delta \simeq 2\pi\zeta$.

Generally for low damping, it is preferable to measure the amplitudes of oscillations of many cycles so that an accurately measurable difference exists. In such a case,

$$\delta = \frac{1}{n} \ln\left(\frac{x_0}{x_n}\right) \quad (2)$$

where x_0 , x_n and n are the amplitudes of first and last cycles and number of cycles, respectively.

1.3.2 Quality Factor (Q)

The half-power point bandwidth method is a frequency-domain method used to determine the damping in terms of quality factor (Q). This method is based on the magnitude curve of the frequency-response function. When a structure is subjected to a forced vibration by a harmonic exciting force, the ratio of maximum dynamic displacement (X_{\max}) at steady-state condition to the static displacement (X_s) under a similar force is called the Q factor.

$$Q = \frac{X_{\max}}{X_s} = \frac{1}{2\zeta} \quad (3)$$

The above equation shows that the Q factor is equal to the reciprocal of twice the damping ratio ζ . Since a structure is excited into resonance at any of its modes, a Q factor can be determined for each mode. Systems with high Q factor have low damping and vice versa.

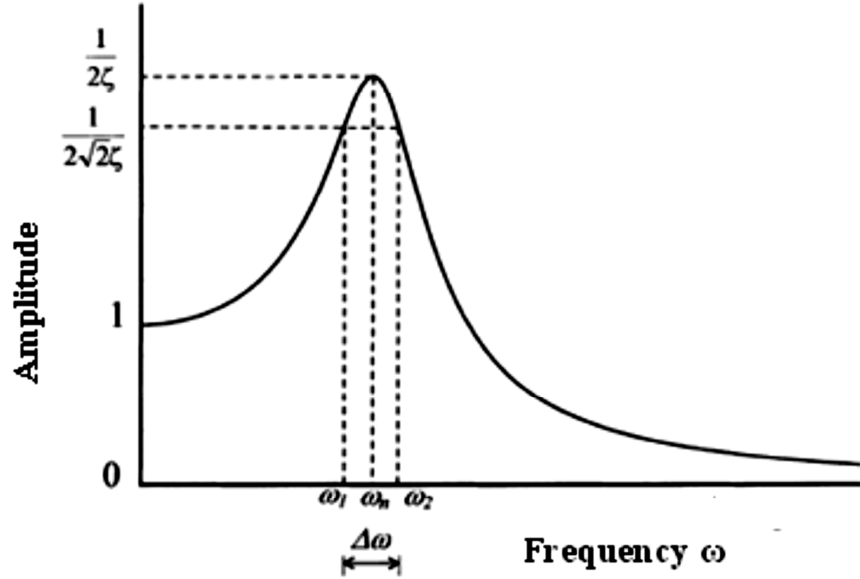


Figure.1 Q-factor method of damping measurement

If the static displacement (X_s) cannot be determined, the Q factor is found out using the half-power point method [1]. The half-power points are those points on the response curve with amplitude 1.2 times the amplitude at resonance as presented in Fig. 1. This method requires very accurate measurement of the vibration amplitude for excitation frequencies in the region of resonance. Once the maximum dynamic displacement (X_{\max}) and resonant frequency (ω) have been located, the so-called half-power points are determined when the amplitude is (X) and the corresponding frequencies on either side of resonant frequencies, ω_1 and ω_2 are determined. Since the energy dissipated per cycle is proportional to the square of amplitude, the energy dissipated is reduced by 50% when the amplitude is reduced by a factor $(1/\sqrt{2})$. Thus the Q factor is modified as:

$$Q = \frac{1}{2\zeta} = \omega_n \frac{n}{\Delta\omega} \quad (4)$$

where $\Delta\omega$ is the frequency bandwidth at the half-power points.

1.3.3 Damping Ratio (ζ)

The damping ratio is another way of measuring damping which shows the decay of oscillations in a system after a disturbance. Many systems show oscillatory behavior when they are disturbed from their position of static equilibrium. Frictional losses damp the system and cause the oscillations to gradually decay to zero amplitude. The damping ratio provides a mathematical means of expressing the level of damping in a system. It is defined as the ratio of the damping constant to the critical damping constant.

The rate at which the motion decays in free vibration is controlled by the damping ratio ζ , which is a dimensionless measure of damping expressed as a percentage of critical damping. Figure 2 displays the free vibration response of several systems with varying levels of damping ratios. It is observed that the amplitude of vibration decays more rapidly as the value of the damping ratio increases.

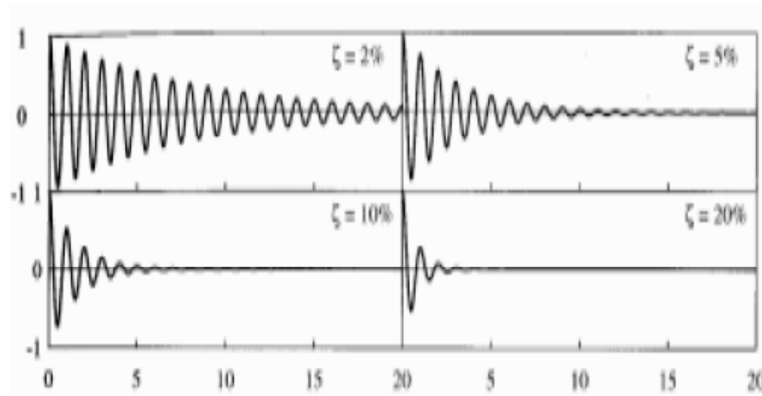


Figure 2 Free vibration of systems with different levels of damping.

1.3.4 Specific Damping Capacity (Ψ)

The damping capacity is defined as the energy dissipated per complete cycle of vibration. The energy dissipation per cycle is calculated from the damping force

It is expressed in the integral for $\Delta U = \oint f \left(\frac{d}{d_x} \right)$ (5)

This is given by the area of the hysteresis loop in the displacement force-plane. The specific damping capacity (Ψ) is defined as the ratio of energy dissipated per cycle of vibration to the total energy of the system. If the initial (total) energy of the system is denoted by U_{\max} , the

specific damping capacity is given by; $N\psi = \frac{\Delta U}{U_{\max}}$

1.3.5 Loss Factor (η)

The loss factor η is the specific damping capacity per radian of the damping cycle and is widely used in case of viscos-elastic damping. This is expressed as;

$$\eta = \frac{\Delta U}{2\pi U_{\max}} \quad (6)$$

It is noted that U_{\max} is approximate equal to the maximum kinetic or potential energy of the system when the damping is low. Finally, the general relationship among various nomenclatures of damping measurement (valid for small values of damping) is given by;

$$1/Q = \psi/2\pi = 2\zeta = \delta/\pi = \eta = \Delta U / [2\pi U] \quad (7)$$

1.4 Linear Problem

Most structural problems are studied based on the assumption that the structure to be analyzed is either linear or nonlinear. In linear systems, the excitation and response are linearly related and their relationship is given by a linear plot as shown in *Fig. 3*. For many cases, this assumption is more often valid over certain operating ranges. Working with linear models is easier from both an analytical and experimental point of view. For beams undergoing small displacements, linear beam theory is used to calculate the natural frequencies, mode shapes and the response for a given excitation.

It is very clear from *Fig. 3* that the linear and nonlinear systems agree well at small values of excitation, while they deviate at higher levels. The nonlinear beam theory is used for larger displacements where the superposition principle is not valid. The linear vibration theory is used when the beam is vibrated at small amplitudes and lower modes of vibration. The present investigation mainly focuses on the study of damping of jointed fixed-fixed beams at lower excitation levels which can be well considered as linear.

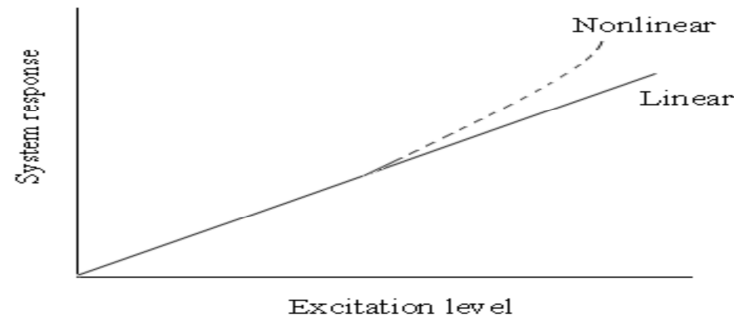


Figure 3 Comparison of Linear and nonlinear systems

1.5 Beam Theories

The beam is one of the fundamental elements of an engineering structure and finds application in structural members like helicopter rotor blades, spacecraft antennae, flexible satellites, airplane wings, gun barrels, robot arms, high-rise buildings, long span bridges, etc. These beam-like structures are typically subjected to dynamic loads. Therefore, studying the static and dynamic response, both theoretically and experimentally, of these structural components under various loading conditions would help in understanding and explaining the behavior of more complex and real structures.

The popular beam theories in use today are: (a) Euler-Bernoulli beam theory and (b) Timoshenko beam theory. Dynamic analysis of beams is generally based on one of the above beam theories. If the lateral dimensions of the beam are less than one-tenth of its length, then the effects of shear deformation and rotary inertia are neglected for the beams vibrating at low frequency. The no-transverse-shear assumption means that the rotation of cross section is due to bending alone. A beam based on such conditions is called Euler-Bernoulli beam or thin beam.

If the cross-sectional dimensions are not small compared to the length of the beam, the effects of shear deformation and rotary inertia are to be considered in the analysis. Timoshenko included

these effects and obtained results in accordance with the exact theory. The procedure presented by Timoshenko is known as thick beam theory or Timoshenko beam theory. The present investigation is based on the assumptions of Euler-Bernoulli beam theory as the beam is vibrated at low frequency and the dimensions of test specimens are much smaller in the lateral directions compared to length, thus satisfying the condition of thin beam theory.

1.6 Modeling of a Structure

It is essential to have a theoretical model to represent a structure in order to study its dynamic characteristics. Theoretical modeling of the present problem considers two approaches using the Euler-Bernoulli beam theory: continuous model approach and finite element model approach.

A continuous model is characterized by a partial differential equation with respect to spatial and time coordinates which is often used for studying simple structures such as a uniform beam. Exact solutions of such equations are possible only for a limited number of problems with simple geometry, boundary conditions and material properties. However, real-life engineering structures are generally very complex in geometry, boundary conditions and material properties. For this reason, normally some kind of other approximate method is needed to solve a general problem. The classical logarithmic decrement method is very popular for measuring damping in the time domain. This method is mostly used for free vibration response of a lightly damped linear system having low and medium frequency range. In this method, the damping is measured for a single frequency oscillation directly from the decay of the system response. It is established that this method is equally applicable to single as well as multiple degrees of freedom systems. In case of multiple degrees of freedom systems, the damping for each mode is separately determined if the decay of initial excitation takes place primarily in one mode of vibration.

1.6.1 Classification of Joints According To Configuration

An important step towards the analysis and representation of the mode of vibration of machine is the analysis of spatial vibration behavior of the structure when vibrating in its resonance frequencies. In order to examine a machine from structural point of view it is necessary to provide a method by which a structural mode is abstracted from a machine. The modular construction system for machine tool has recently become important not only to rationalize their design and manufacturing procedure but also to evolve a feasible manufacturing system. Fundamental shape, main cross-sectional shape and function of structural modules and relation between adjacent structural configuration shows that a machine consists of many elementary aggregate. This hierarchical property of machine structure suggests the possibility of defining a concrete model suitable for each joint in machine tool. Following fundamental characteristics of the joint are to be considered when replacing machine tool joints by mathematical model:

- (1) The static stiffness of structures with joints is considerably lower than that of the equivalent solid structures and joint stiffness show the non-linear characteristics.
- (2) The damping capacity of jointed structures is higher than that of equivalent solid one, but the natural frequency of jointed structures is less as compared to solid one.
- (3) The characteristics mentioned above are in large dependence on the stiffness ratio of joint surrounding.

Sliding joint

Here joint displacement to sum of the roughness ratio is smaller than unity. The ratio also increases with an increasing interface pressure. In plain slide-ways the dynamic characteristics are mainly determined by damping caused by friction, the mass of the carriage and the stiffness and damping of the drive. The stiffness and the damping of the practical fabricated structures are not always linear because of the existence of a certain preload is considered. The damping caused by friction is non-linear and may be either positive or negative which means either stable sliding or self-excited oscillations (stick-slip). Measurement shows that damping depends upon slide ways materials, velocity, lubricant and mass. Mechanism of damping in a joint is not merely due to friction but is a complex one of micro and macro friction and cyclic plastic deformation is likely to be predominant mechanism to which energy dissipation could be attributed.

(1) Macro-slip involving frictional damping

(2) Micro-slip involving very small displacement of asperities with respect to other surface.

1.6.2 Damping Due To Sandwich Construction

The forced vibration of beams and plates can be reduced by inserting a layer of damping material at attachment point and by permitting some motion to take place. Core thickness equal to or greater than the thickness of the metal constraining layer can provide high overall damping. Artificial means of effecting interfacial damping is envisaged namely bolted, riveted, welded, laminated adhesive joint to serve the dual purpose of fastening and damping the vibration. Structural member can be joined by adhesive, fastener and welding method

1.7 Different Techniques of Damping

(i) Unconstrained construction:

Layer of viscoelastic layer is bonded to elastic one. In this case the viscoelastic layer to elastic one, the viscoelastic layer is subjected to alternate extension and compression as the elastic layer to which it is bonded experiences flexural vibrations, mostly applied to finished material structure like automobile bodies, ship hulls, and air craft skin.

(ii) Constrained construction:

Viscoelastic layer is sandwiched between two elastic layers. Such an arrangement vibrating in bending would cause shear strain in viscoelastic layer, causing energy dissipation. This type used in printed circuit board for air craft missiles, mounting platforms for electronic and guidance apparatus, air craft and missile structure, building bridges, ship engine. Constrained type of treatment is seen to be more beneficial in practice as it is seen to be more beneficial in practice as it is seen to provide more damping for the same total weight of structure. Adhesive layer in the joint forms an equivalent solid coupling. Cyclic damping produced in thin layers of dissipative material placed between two rigid surfaces is inversely proportional to adhesive layer thickness.

(iii) Laminated Construction:

Damping in plate type of structure can be significantly increased by using laminated plates correctly fastened to allow interfacial slip during vibration. We know that considerable damping can be achieved by using viscoelastic material in structures; the damping capacity of material is both frequency and temperature sensitive to a much greater extent than that found in friction, so that their use in the condition of changing temperature and frequency is limited. Viscoelastic material is an extra structural element, so that further advantage of frictional damping is that it

does not require extra space for damping material to be filled in the structure. In this case panel of thickness t is replaced by n laminates of total thickness T (each of thickness T/n). The laminates were fastened together in such a way that as the panel vibrates interfacial slip occurs between laminates, thus giving rise to frictional damping. This can be achieved by riveting. Some suggestions are given for interface preparation and its effects on frictional damping in joint. If fretting occurs in a joint at least two undesirable effects may occur.

(i) Fretting may introduce serious corrosion damage within the joint and initiate crack with ultimate fatigue failure.

(ii) The fretting action may allow the joint to drift from any present clamping condition or even cause jamming at critical clearance.

Shot peening and blasting both increase surface roughness and reduce surface damage compared with ground surface, while metal spray show little surface damage but introduce some instability in joint. However cyanide hardened surface show very stable condition with slight surface damage without impairing energy dissipation capability of joint. As the material damping within the structural members is of low magnitude, various other techniques are used to improve the damping capacity of structures. These are: (i) Use of constrained/unconstrained viscoelastic layers, (ii) fabrication using a multi-layered sandwich construction, (iii) use of stress raisers, (iv) Insertion of special high-elasticity inserts in the parent structure, (v) application of spaced damping techniques, (vi) Use of a viscous fluid layer, (vii) use of bonded joints and (viii) fabricating layered and jointed structures.

1.8 Various Types of Jointed Structures

RIVETED:

A rivet is a perpetual mechanical fastener. Before being mounted a rivet involves in a smooth cylindrical shaft with a head on one end. The end opposite the head is called the buck-tail. On connection the rivet is placed in a pierced or pre-drilled hole, and the tail is upset, or bucked (i.e. deformed), so that it expands to about 1.5 times the original shaft diameter, holding the rivet in place. To extricate between the two ends of the rivet, the unique head is called the factory head and the distorted end is called the shop head or buck-tail.

Because there is effectually a head on each end of an installed rivet, it can support tension loads (loads parallel to the axis of the shaft); however, it is much more capable of supporting shear loads (loads perpendicular to the axis of the shaft). Bolts and screws are better matched for tension applications.

Fastenings used in traditional wooden boat building, like copper nails and clinch bolts, work on the same standard as the rivet but were in use long before the term rivet came about and, where they are recollected, are usually classified among the nails and bolts respectively.

BOLTED:

Bolted joints are one of the most collective elements in construction and machine design. They entail of fasteners that capture and join other parts, and are protected with the mating of screw threads. There are two chief types of bolted joint designs. In one method the bolt is stiffened to a calculated clamp load, usually by smearing a measured torque load. The joint will be intended

such that the clamp load is never overwhelmed by the forces acting on the joint (and therefore the joined parts see no relative motion). The other type of bolted joint does not have an intended clamp load but depends on the shear strength of the bolt shaft. This may comprise clevis linkages, joints that can change, and joints that depend on a locking mechanism (like lock washers, thread adhesives, and lock nuts). The clamp load, also called preload, of a clasp is created when a torque is smeared, and is commonly a percentage of the fastener's resilient strength; a fastener is contrived to various values that define, among new things, its asset and clamp load. Torque charts are accessible to identify the required torque for a fastener created on its property class or grade. When a fastener is tightened, it is pushed and the parts being joined are compressed; this can be modeled as a spring-like assemblage that has a non-intuitive dissemination of strain. External forces are intended to act on the secured parts appealing than on the fastener, and as time-consuming as the forces acting on the clasped parts do not exceed the clamp load, the fastener is not subjected to any increased load.

WELDED:

Welding joints are shaped by welding two or more work pieces, made of metals or plastics, according to a precise geometry. The most common types are butt and lap joints; there are various minor used welding joints counting flange and corner joints. Here we used tack weld which is a temporary fastener. The tack weld is a little small weld that is not designed to be of any structural value. The tack weld is just a one second squash on the trigger. It would be much easier for me to only slog off these small tack welds instead of a big long weld bead. So you can see here what tack welding is and what it would be used for.

1.9 Aims and Objectives

Built-up structures are generally fabricated using many types of fasteners such as bolted, riveted and welded joints. It is the well-known fact that the improvement in damping due to the provision of welded joints is not appreciable compared to the use of bolted or riveted joints. Therefore, the use of welded joints is usually avoided in structural applications where higher damping is the main criterion. In case of bolted and riveted joints, the fundamental mechanism of damping may be same, but they differ in their functional aspects. For example, the parameters such as interface pressure distribution characteristics, zone of influence and preload are not same in both cases. . However, a little amount of research has been reported till date on the welded joints. The use of welding in such applications is cheaper compared to other fasteners thereby giving low assembly cost. Since the zone of influence differs in both cases, the relative spacing among the joints will be different thereby changing the relative dynamic slip at the interfaces. These facts suggest that the damping action for both cases is not same. Further, the axial load on a bolt can be varied by applying the tightening torque as per the clamping requirements of the structure whereas the preload in a rivet is constant and cannot be changed in the latter part of the design. Consequently, it is highly desirable that the machine members, building structures and industries can definitely make use of jointed construction for the improvement of damping without sacrificing strength where vibration is encountered. Moreover, the basic mechanism of energy loss due to interface friction and slip is same in case of all the fasteners. Therefore, an attempt has been made in the present investigation to study the mechanism of interface slip damping considering the above concept for layered and these jointed structures.

CHAPTER-2

LITERATURE SURVEY

Structural damping is widely used for creating of many structures. Although an ample amount of work has been reported on the study of damping in rivet and bolt structures with non-uniform pressure distribution at the interfaces, no generalized theory has been established for these beams with uniform pressure distribution at the interfaces. Most engineering designs are built up by connecting structural components through mechanical connections. Such assembled designs need sufficient damping to limit excessive vibrations under dynamic loads. Damping in such designs mainly starts from two sources. One is the internal or material damping which is innately low [1] and the other one is the structural damping due to joints [2]. The behind one offers a best source of energy dissipation, thereby sufficiently compensates the low material damping of structures. It is estimated that structures consisting of bolted or riveted members contribute about 90% and rest by others of the damping through the joints [3]. The work in this thesis is oriented towards the use of mechanical systems fabricated in layers jointed with them for achieving increased damping.

As discussed in the preceding paragraph, the arrangement of layers in association with joints encourages large damping in built-up structures. These connections are identified as a good source of energy dissipation and mostly affect the dynamic behavior in terms of natural frequency and damping [4, 5]. This structural damping offers excellent potential for large energy dissipation is associated with the interface shear of the joint. It is thus identified that the provision of joints can effectually contribute to the damping of all fabricated structures. Although most of the connate damping occurring in real structures arises in the joints, but a little effort has been made to study this source of damping because of complex mechanism occurring at the interfaces due to relative slip, coefficient of friction and pressure distribution

characteristics. It is therefore important to focus the contemplation to study these parameters for accurate assessment of the damping capacity of structures.

Over the past few decades, most of the work has been done in the area of micro- and macro-slip phenomena [6, 7]. These concepts are utilized to study the dynamic behavior of jointed structures having friction contact [8-15]. This model is generally adopted when the normal load at the interface is small. On the other hand, many researchers [13, 14] have utilized the micro-slip concept considering the friction surface as an elastic body. In this case, the interface undergoes partial slip at high normal load. Masuko et al. [16] and Nishiwaki et al. [17, 18] have found out the energy loss in jointed cantilever beams considering micro-slip and normal force at the interfaces. Olofsson and Hagman [19] have shown that the micro-slip at the contacting surfaces occur when a best frictional load is applied. They have also presented a model for micro-slip between the flat smooth and rough surfaces covered with ellipsoidal elastic bodies.

The role of friction is of paramount significance in controlling the dynamic characteristics of engineering structures. This may be undesirable or desirable depending on the type of applications. Friction is often considered unique in the design of moving parts. On the other hand, this is desirable in fabricated structures for effective energy dissipation. Therefore, this concept of design is always acknowledged in assembled structures requiring high damping. The friction at the jointed interfaces arises when the layers experience relative movement under transverse vibration. The Coulomb's law of friction is widely used to represent the dry friction at the contacting surfaces. The friction in a joint arises from shearing between the parts and is governed by the tension in the bolt/rivet, surface properties and type of materials in contact [20]. Den Hartog [21] has analytically solved the steady state response of a simple friction-damped

system with dual Coulomb and viscous friction. Reviews on the effects of joint friction on structural damping in built-up structures have been presented by many researchers [22, 5, 23]. Their findings have shown that the friction in structural joints is regarded as a major source of energy dissipation in assembled structures.

The nature of pressure distribution through a beam layer is another important aspect affecting the damping capacity of jointed structures. Several workers have tried over the years to know the actual design of pressure distribution at the interfaces due to the clamping action on the joint. Almost all previous researchers have seen the joints by assuming a uniform pressure profile without considering the effects of surface irregularities and asperities [16-18]. In fact, many authors [24-29] have conducted experiments to know the exact distribution characteristics. These experiments have confirmed that the interface pressure is constant in original situation. In particular, Gould and Mikic [28] and Ziada and Abd [29] have reported that the pressure distribution at the interfaces of a bolted joint is parabolic in nature circumscribing the bolt which is approximately 3.5 times the bolt diameter. Recently, Nanda and Behera [30] have developed a theoretical session for the pressure distribution at the interfaces of a bolted joint by curve fitting the earlier data reported by Ziada and Abd [31]. They have obtained an eighth order polynomial even function in terms of normalized radial distance from the Centre of the bolt such that the function assumes its maximum value at the Centre of the bolt and decreases radially away from the bolt. They have used Dunn's curve fitting software to calculate the perfect spacing between bolts that would result in a uniform interfacial pressure distribution along the entire length of the beam. Using exact spacing of 2.00211 times the diameter of the connecting bolts, Nanda and Behera have been successful in simulating uniform interface pressure over the length of the beam. Goodman and Klumpp [2] examined the energy dissipation due to slip at the interfaces of

a laminated beam. In fact, previous investigators such as; Cockerham and Symmons [32], Hess et al. [33] and Guyan et al. [34] considered various friction and excitation models, while Barnett et al. [35] and Maugin et al. [36] considered interfacial slip waves between two surfaces for the measurement of damping capacity of structures. Studies by researchers such as; Goodman [37], Earles [38], Murty [39] have shown that the energy dissipation at the joints occur due to frictional energy loss at the interfaces which is more than the energy loss at the support. In fact following the work of Goodman and Klumpp, early workers, such as Masuko et al [40], Nishiwaki et al [41], and Motosh [42] studied the damping capacity of layered and bolted structures assuming uniform intensity of pressure distribution at the interfaces of such structures. However, their work is limited to the layered and jointed symmetric structures.

Hansen and Spies [43] investigated the structural damping in laminated beams due to interfacial slip. They analyzed a two layered plate model with an assumption that there exists an adhesive layer of negligible thickness and mass between the two layers such that some amount of micro-slip originates at the frictional interfaces which contributes to the damping. They have also shown that the restoring force is developed by this adhesive medium and is proportional to the interfacial micro-slip. The effect of non-uniform interface pressure distribution on the mechanism of slip damping for layered beams has also been examined recently by Damisa et al. [44], but their analysis is limited to the case of static load. Damisa et al. [45] also examined the effect of non-uniform interface pressure distribution on the mechanism of slip damping for layered beams under dynamic loads. Though these researchers considered the in-plane distribution of bending stresses but all the analysis is limited to the symmetric structures with single interface. Many comprehensive review papers on joints and fasteners have appeared in recent years. The small, localized motions during micro-slips result in energy losses at the joint,

which is perceived as localized damping of the structure. Berger [46] has studied the effect of micro-slip on passive damping of a jointed structure. Beards [47] performed a series of experiments showing that the damping in joints is much larger than the material damping.

Mayer and Gaul [48] discussed the segment- to-segment contact elements of a structure having both linear and nonlinear constitutive contact behavior in normal and tangential directions, including nonlinear micro-slip behavior. Further investigations into joints have been undertaken at Sandia National Laboratories [49, 50], aimed at identifying the physics of joint interfaces. A series of closely controlled experiments has established that there exists a power-law relationship between input force and energy dissipated per cycle [51], and further experimental results identified the regions of micro-slip. Further work at Sandia examined the use of Iwan models [52] to describe the dynamics of joints [53]. The Iwan model consists of a continuum network of springs and sliders, with the break-free forces of the sliders being described as a probability distribution function. Different distribution functions lead to different power laws in the diagrams of input force vs. energy dissipated per cycle. Although a lot of work has been carried out on the damping capacity of bolted structures, little work has been reported on the mechanism of damping in layered and jointed welded structures. Recently, Singh and Nanda [54] proposed a method to evaluate the damping capacity of tack welded structures. They established that with the increase in the number of tack welds the damping capacity decreases.

CHAPTER – 3

THEORETICAL ANALYSIS

It is generally recognized that the damping capacity of the jointed beam and the sandwiched beam may be determined by the frictional loss energy caused by the slip at the interfaces of both steel beams and the slip between the steel beams and the sandwiched viscoelastic material. The slip found between the interfaces of jointed beam however is very small and shows very complicated characteristics, and moreover the coefficient of friction in this case may be considered smaller than the macroscopic coefficient of friction used widely in the field.

The logarithmic damping decrement, a measure of damping capacity of layered and jointed structures, is usually determined by the energy principle taking into account the relative dynamic slip and the interfacial pressure distribution at the contacting layers. The logarithmic damping decrement is evaluated theoretically for the beams with different end conditions such as; fixed-free and fixed-fixed respectively.

3.1 Interface Pressure Distribution

A layered and jointed construction is made by means of rivets that hold the members together at the interfaces. Under such circumstances, the profile of the interface pressure distribution assumes a significant role, especially in the presence of slip, to dissipate the vibration energy. Consequently, it is necessary to examine the exact nature of the interface pressure profile and its magnitude across a beam layer for the correct assessment of the damping capacity in a jointed structure. This pressure distribution at the interfaces is due to the clamping of the contacting members. When two or more members are pressed together by riveting, a circle of contact will be formed around the rivet and bolt with a separation taking place at a certain distance from the rivet hole as shown in figure below.

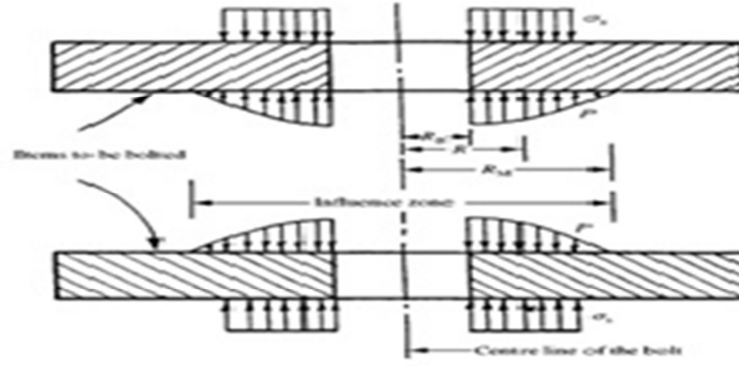


Figure 4 Free body diagram of bolted joint showing influence zone

The contact between the connecting members develops an interface pressure whose exact nature and magnitude across the beam layer is very important for the correct assessment of damping capacity of a jointed structure. As established, the contact pressure at the jointed interface is non-uniform in nature being maximum at the rivet hole and decreases with the distance away from the rivet. This allows localized slipping at the interfaces while the overall joint remains locked. Minakuchi et al. [35] have found that the interface pressure distribution due to this contact is parabolic with a circular influence zone circumscribing the rivet with diameter equal to 4.125, 5.0 and 5.6 times the diameter of the connecting rivet for thickness ratio of 2.0, respectively.

3.1.1 Determination of Pressure Distribution at the Interfaces for Riveted and Bolted Joints

The interface pressure distribution under each rivet in a non-dimensional polynomial for layered and jointed structures is assumed as

$$P/\sigma_s = C_1(R/R_B)^{10} + C_2(R/R_B)^8 + C_3(R/R_B)^6 + C_4(R/R_B)^4 + C_5(R/R_B)^2 + C_6 \quad (8)$$

where P , σ_s , R and R_b are the interface pressure, surface stress on the layered and jointed structure due to riveting, any radius within the influencing zone and radius of the connecting rivet, respectively and constants 1C to 6C of the polynomial are evaluated from the numerical data of Minakuchi et al. [35] by curve fitting using MATLAB software as shown. The surface stress σ_s depends upon the initial tension on the rivet (P) and the area under a rivet head (A') and is evaluated from the relation

$$P / \sigma_s = P / A' \quad (9)$$

The distance between the rivets has been reduced in order to achieve the uniform pressure conditions.

The above equation is an even function and a tenth order polynomial in terms of the normalized radial distance from the center of the rivet such that the function assumes its maximum value at the center of the rivet and decreases radially. It is evident that apart from the last two terms, values of the coefficients are relatively insignificant. This suggests for a linear profile for the pressure distribution across the interface. Damisa et al. [32] have used linear pressure profile in their analysis as an approximation. But a higher order polynomial for non-uniform interface pressure distribution has been used in the present investigation in order to obtain a good accuracy.

3.2 Dynamic Equations of Free Transverse Vibration of Fixed-Fixed Beams.

3.2.1 Introduction

This chapter gives a detailed description of the theoretical analysis by classical energy approach for determining the damping capacity in layered and jointed fixed-fixed beam with welded joints. A fixed-fixed beam model representing a continuous system based on the Euler-Bernoulli beam theory has been used for deriving the necessary formulation.

3.3 Dynamic equations for free transverse vibration on various joint structures.

The beam vibration is governed by partial differential equations in terms of spatial variables x and time variable t . Thus, the governing differential equation for free vibration is given by:

$$EI \frac{d^4 y}{dx^4} + \rho A \frac{d^2 y}{dt^2} = 0 \quad (10)$$

Where E , I , ρ and A are modulus of elasticity, second moment of area of the beam, mass density and cross-sectional area of the beam respectively. The free vibration given by eq. 10 contains four spatial derivatives and hence requires four boundary conditions for getting a solution. The presence of two time derivatives again requires two initial conditions, one for displacement and another for velocity.

Eq. (11) is solved by method of separation of variables. The displacement $y(x, t)$ is written as the product of two function, one depends on only x and other depends only on t . Thus the solution is expressed as:

$$y(x, t) = X(x) \times F(t) \quad (11)$$

Where $X(x)$ and $F(t)$ are the space and time function respectively.

Substituting eq. (11) into eq. (10) and rearrange results;

$$EIF(t) \frac{d^4 X}{dx^4} = -\rho A X(x) \frac{d^2 T}{dt^2} \quad (12)$$

Dividing eq. (12) by $X(x)F(t)$ on both sides, variables are separated as;

$$\frac{\frac{d^2 T}{dt^2}}{T(t)} = -\frac{EI}{\rho A} \frac{\frac{d^4 X}{dx^4}}{X(x)} = \omega_n^2 \quad (13)$$

Where the term ω_n^2 is the separation constant, representing the square of natural frequency.

This equation yields two ordinary differential equations.

The first one is given as;

$$\frac{d^4 X}{dx^4} - \lambda^4 X(x) = 0 \quad (14)$$

$$\text{Where } \lambda^4 = \frac{\rho A}{EI} \omega_n^2 \quad (15)$$

The required solution of eq. (15) is simplified as;

$$X(x) = A_1 \sin \lambda x + A_2 \cos \lambda x + A_3 \sinh \lambda x + A_4 \cosh \lambda x \quad (16)$$

Where constant A_1 , A_2 , A_3 and A_4 are determined from the boundary conditions of fixed-fixed beam.

The second equation is given as;

$$\frac{d^2 T}{dt^2} + \omega_n^2 T(t) = 0 \quad (17)$$

This is the similar free vibration expression for an un-damped single degree of freedom system having the solution

$$T(t) = A \cos \omega_n t + B \sin \omega_n t \quad (18)$$

Dynamic equation for rivet joints is expressed by inserting the values of A and B

$$y(x, t) = Y(x) \frac{y_0}{y(l/2)} \cos \omega_n t \quad (19)$$

Substituting the expression for space and time function as given by eq. (17) and eq. (18) into eq.

(12), the complete solution for the deflection of a beam at any section is expressed as;

$$y(x, t) = (A_1 \sin \lambda x + A_2 \cos \lambda x + A_3 \sinh \lambda x + A_4 \cosh \lambda x) \times (A_5 \cos \omega_n t + A_6 \sin \omega_n t) \quad (20)$$

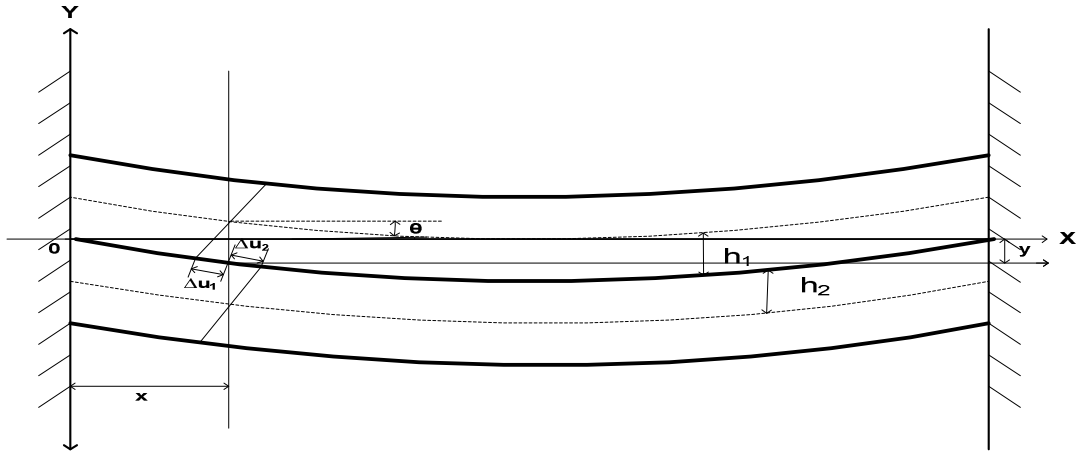


Figure 5 variation of damping in a fixed-fixed beam

3.3.1 Evaluation of Constants A_1, A_2, A_3 and A_4

The boundary conditions for the fixed-fixed beam are given as;

$$\text{At } x = 0; \quad X(0) = 0; \quad X'(0) = 0;$$

$$\text{At } x = L; \quad X(L) = 0; \quad X'(L) = 0;$$

Writing the expression of space function as given in eq. (19) and its first derivative are written as;

$$X(x) = A_1 \sin \lambda x + A_2 \cos \lambda x + A_3 \sinh \lambda x + A_4 \cosh \lambda x \quad (21)$$

$$X'(x) = \lambda(A_1 \cos \lambda x - A_2 \sin \lambda x + A_3 \cosh \lambda x + A_4 \sinh \lambda x) \quad (22)$$

Putting the boundary conditions, eq. (22) is reduced to

$$X(0) = A_1 + A_3 = 0; \quad (23)$$

$$X'(0) = A_2 + A_4 = 0; \quad (24)$$

$$X(L) = A_1 \sin \lambda L + A_2 \cos \lambda L + A_3 \sinh \lambda L + A_4 \cosh \lambda L = 0 \quad (25)$$

$$X'(x) = \lambda(A_1 \cos \lambda L - A_2 \sin \lambda L + A_3 \cosh \lambda L + A_4 \sinh \lambda L) = 0 \quad (26)$$

$$\text{i.e., } A_1 \cos \lambda L - A_2 \sin \lambda L + A_3 \cosh \lambda L + A_4 \sinh \lambda L = 0 \quad (27)$$

The eq. (24) can be represented in a matrix form as;

$$\begin{bmatrix} 0 & 1 & 0 & 1 \\ 1 & 0 & 1 & 0 \\ \sin \lambda L & \cos \lambda L & \sinh \lambda L & \cosh \lambda L \\ \cos \lambda L & -\sin \lambda L & \cosh \lambda L & \sinh \lambda L \end{bmatrix} \begin{bmatrix} A_1 \\ A_2 \\ A_3 \\ A_4 \end{bmatrix} = \begin{bmatrix} 0 \\ 0 \\ 0 \\ 0 \end{bmatrix}$$

To get a non-trivial solution, setting the determinant equal to zero;

$$\begin{vmatrix} 0 & 1 & 0 & 1 \\ 1 & 0 & 1 & 0 \\ \sin \lambda L & \cos \lambda L & \sinh \lambda L & \cosh \lambda L \\ \cos \lambda L & -\sin \lambda L & \cosh \lambda L & \sinh \lambda L \end{vmatrix} = 0$$

The characteristic equation is given as;

$$\cosh (\lambda L) \times \cos (\lambda L) = 1 \quad (29)$$

The constant A_2, A_3 and A_4 are dependent parameter but A_1 is an independent parameter. A_1 may have any values. Taking $A_1 = 1$, the values of A_2, A_3 and A_4 are found as;

$$A_2 = \left(\frac{\sinh \lambda L - \sin \lambda L}{\cos \lambda L - \cosh \lambda L} \right); \quad A_3 = -1; \quad A_4 = -\left(\frac{\sinh \lambda L - \sin \lambda L}{\cos \lambda L - \cosh \lambda L} \right); \quad A_1 = 1 \quad (30)$$

Now space function given by eq. (3.6) is modified as;

$$X(x) = \sin \lambda x + \left(\frac{\sinh \lambda L - \sin \lambda L}{\cos \lambda L - \cosh \lambda L} \right) \cos \lambda x - \sinh \lambda x - \left(\frac{\sinh \lambda L - \sin \lambda L}{\cos \lambda L - \cosh \lambda L} \right) \cosh \lambda x \quad (31)$$

$$\text{i.e, } X(x) = \frac{(\sin \lambda x - \sinh \lambda x)(\cos \lambda L - \cosh \lambda L) + (\cos \lambda x - \cosh \lambda x)(\sinh \lambda L - \sin \lambda L)}{(\cos \lambda L - \cosh \lambda L)} \quad (32)$$

This equation gives the different mode shapes of vibration.

3.3.2 Evaluation of constants A_5 and A_6

The general expression of deflection at any section of beam is given by;

$$Y(x, t) = X(x) \times (A_5 \cos \omega_n t + A_6 \sin \omega_n t) \quad (33)$$

Taking the derivative with respect to time, the above equation reduced to;

$$y'(x, t) = X(x) \times (-A_5 \omega_n \sin \omega_n t + A_6 \omega_n \cos \omega_n t) \quad (35)$$

The velocity of deflection at the mid-span of the beam is zero.

$$\text{i.e., } y' \left(\frac{L}{2}, 0 \right) = 0, \text{ this yields } A_6 = 0; \quad (37)$$

Hence the eq. (35) is reduced to;

$$Y(x, t) = X(x) \times (A_5 \cos \omega_n t) \quad (38)$$

The deflection at the mid-span of the beam is taken equal to $X\left(\frac{L}{2}\right)$ and substituting the same in eq. (37), we obtained;

$$y\left(\frac{L}{2}, 0\right) = X\left(\frac{L}{2}\right) \times A_5 \quad (39)$$

$$\text{i.e., } A_5 = \frac{y\left(\frac{L}{2}, 0\right)}{X\left(\frac{L}{2}\right)}; \quad (40)$$

Substituting the values of A_5 in eq. (36), the final equation for the deflection is found to be;

$$y(x, t) = X(x) \times \left[\frac{y\left(\frac{L}{2}, 0\right)}{X\left(\frac{L}{2}\right)} \right] (\cos \omega_n t) \quad (41)$$

$$y(x, t) = \left[\frac{(\sin \lambda x - \sinh \lambda x)(\cos \lambda L - \cosh \lambda L) + (\cos \lambda x - \cosh \lambda x)(\sinh \lambda L - \sin \lambda L)}{(\cos \lambda L - \cosh \lambda L)} \right] \left[\frac{y\left(\frac{L}{2}, 0\right)}{X\left(\frac{L}{2}\right)} \right] \cos \omega_n t \quad (42)$$

This is the generalized deflection equation at any section of a fixed-fixed beam.

3.3.3 Evaluation of relative dynamic slip

The relative slip at the interface in the presence of friction during the vibration is given as;

$$u_r(x, t) = \alpha u(x, t) = 2 \alpha h \tan \left[\frac{\partial y(x, t)}{\partial x} \right] \quad (43)$$

Where α = slip ratio

h = thickness of the beam

$y(x, t)$ = Deflection at a distance 'x' from the fixed end

$u(x, t)$ = *dynamic slip without friction*

3.3.4 Analysis of energy dissipated

The energy is dissipated due to the friction and relative dynamic slip at the interface is given by;

$$E_{loss} = 2 \int_0^{\frac{\pi}{\omega_n}} \int_0^{\frac{L}{2}} \mu p b \left[\left\{ \frac{\partial u_r(x, t)}{\partial t} \right\} \right] dx dt \quad (44)$$

Where μ = coefficient of kinematic friction

p = uniform pressure distribution at the interface

L = length of the beam

ω_n = natural frequency of vibration

The strain energy per half cycle of vibration is given by;

$$E_{ne} = \left(\frac{192EI}{L^3} \right) y^2 \left(\frac{L}{2}, 0 \right) \quad (45)$$

where E , $\left[I = b \frac{(4h)^3}{12} \right]$ and $y(l/2,0)$ are the modulus of elasticity, cross-sectional moment of inertia and transverse deflection at the midpoint of the fixed-fixed beam for rivets , respectively

$$\text{where } \frac{E_{LOSS}}{E_{NET}} = \left[\frac{8\mu b h \alpha y(\frac{l}{2},0)}{192(\frac{EI}{l^3})y^2(\frac{l}{2},0)} \right] \quad (46)$$

Replacing $192EI/l^3 = k_f$ i.e., the static bending stiffness of the layered and riveted cantilever beam, the above equation (42) reduces to

$$\frac{E_{LOSS}}{E_{NET}} = \left[\frac{8\mu b h p \alpha}{k_f y(\frac{l}{2},0)} \right] \quad (47)$$

where k_f is the static bending stiffness of the fixed-fixed beam.

Similarly the energy dissipated for bolted joints and the energy loss due to frictional force at the interfaces per half-cycle of vibration is given by;

$$E_{LOSS} = \int_0^{\frac{\pi}{\omega_n}} \int_0^1 \mu p b \left[\left\{ \frac{\partial u_r(x,t)}{\partial t} \right\} dx dt \right] \quad (48)$$

The energy dissipated for welded joints is given by

$$I = \frac{b(2h)^3}{12}, \text{ cross-sectional moment of inertia of the beam}$$

$$y\left(\frac{l}{2}, 0\right) = \text{transverse deflection at the mid-point of the fixed-fixed beam}$$

Substituting eq. (41) into eq. (42) and is given by;

$$E_{loss} = 4 \propto h\mu pb \int_0^{\frac{\pi}{\omega_n}} \int_0^{\frac{L}{2}} \left[\frac{\partial \left\{ \tan \left(\frac{\partial y(x,t)}{\partial x} \right) \right\}}{\partial t} \right] dx dt \quad (49)$$

The slop is very small i.e. $\tan \left(\frac{\partial y(x,t)}{\partial x} \right) = \frac{\partial y(x,t)}{\partial x}$;

Hence eq. (44) reduced to

$$E_{loss} = 4 \propto h\mu pb \int_0^{\frac{\pi}{\omega_n}} \int_0^{\frac{L}{2}} \left\{ \partial^2 y(x,t) / \partial x \partial t \right\} dx dt \quad (50)$$

The ratio of dissipated energy and strain energy is found out dividing eq. (46) by eq. (47) is given by;

$$\frac{E_{loss}}{E_{ne}} = \left[\frac{4\propto h\mu pb}{\left(\frac{192EI}{L^3} \right) y^2 \left(\frac{L}{2}, 0 \right)} \right] \int_0^{\frac{\pi}{\omega_n}} \int_0^{\frac{L}{2}} \left\{ \partial^2 y(x,t) / \partial x \partial t \right\} dx dt \quad (51)$$

Substituting the boundary and initial conditions eq. (51) reduced to

$$\frac{E_{loss}}{E_{ne}} = \frac{4\propto h\mu pb y \left(\frac{L}{2}, 0 \right)}{\left(\frac{192EI}{L^3} \right) y^2 \left(\frac{L}{2}, 0 \right)} \quad (52)$$

$$or, \frac{E_{loss}}{E_{ne}} = \frac{4\propto h\mu pb y \left(\frac{L}{2}, 0 \right)}{K_s y^2 \left(\frac{L}{2}, 0 \right)} \quad (53)$$

Where K_s = static bending stiffness of fixed-fixed beam.

3.3.5 Evaluation Of Damping Ratio

The damping ratio, ψ , is expressed as the ratio of energy dissipated due to the relative dynamic slip at the interfaces and the total energy introduced into the system for rivets is found to be

$$\psi = \left[\frac{E_{loss}}{E_{loss} + E_{net}} \right] = \frac{1}{\left[1 + \frac{E_{net}}{E_{loss}} \right]} \quad (54)$$

where, E_{loss} and E_{ne} are the energy loss due to interface friction and the energy introduced during the unloading process Putting the values of $\frac{E_{loss}}{E_{ne}}$

$$\psi = \frac{1}{1 + \left[\frac{ky(\frac{l}{2}, 0)}{8\mu b p h \alpha} \right]} \quad (55)$$

$$\psi = \frac{1}{1 + \left[\frac{ky(\frac{l}{2}, 0)}{2\mu b p \alpha h} \right]} \quad (56)$$

The above equations are used for calculating the damping ratio for the three joint structures.

3.3.6 Logarithmic decrement

Logarithmic decrement(δ), a measure of damping capacity, is defined as the natural logarithm of the ratio of two consecutive amplitudes in a given cycle.

$$\delta = \frac{1}{n} \ln \left(\frac{x_0}{x_n} \right) \quad (57)$$

Where x_0 = amplitude of vibration of first cycle

x_n = amplitude of vibration of last cycle

n = number of cycles

Logarithmic decrement can also be written as;

$$\delta = \frac{1}{2} \left(\frac{E_{\text{loss}}}{E_{\text{ne}}} \right) \quad (58)$$

The logarithmic decrement for rivet joints is given as

$$\delta = \frac{1}{n} \ln \left(\frac{a_n}{a_{n+1}} \right) = \left[\ln \left\{ \frac{1}{1 - \psi} \right\} \right] / 2 \quad (59)$$

By simplifying the above equation we get

$$\delta = \frac{1}{2} \ln \left[1 + \frac{8\mu\alpha p b h}{k_y \left(\frac{l}{2}, 0 \right)} \right] \quad (60)$$

Similarly the logarithmic decrement for bolted joints $\mu\alpha$ is assumed to be constant and has been found out from the experimental results for logarithmic damping decrement as

$$\delta = \frac{1}{2} \ln \left[1 + \frac{8\mu\alpha p b h}{k_y \left(\frac{l}{2}, 0 \right)} \right] \quad (61)$$

$$\delta = \left[\frac{2\alpha h \mu p b y \left(\frac{l}{2}, 0 \right)}{K_s y^2 \left(\frac{l}{2}, 0 \right)} \right] \quad (62)$$

CHAPTER – 4

EXPERIMENTATION

4.1 Experimental Set-Up

In order to evaluate the effect of different parameters on damping capacity of various types of riveted joint beams, experiments were carried out with a simple experimental set –up.





Figure 6 Set up and details of mild steel specimens used in the experiment for the thickness ratio 1.0 for riveted, bolted and welded joints

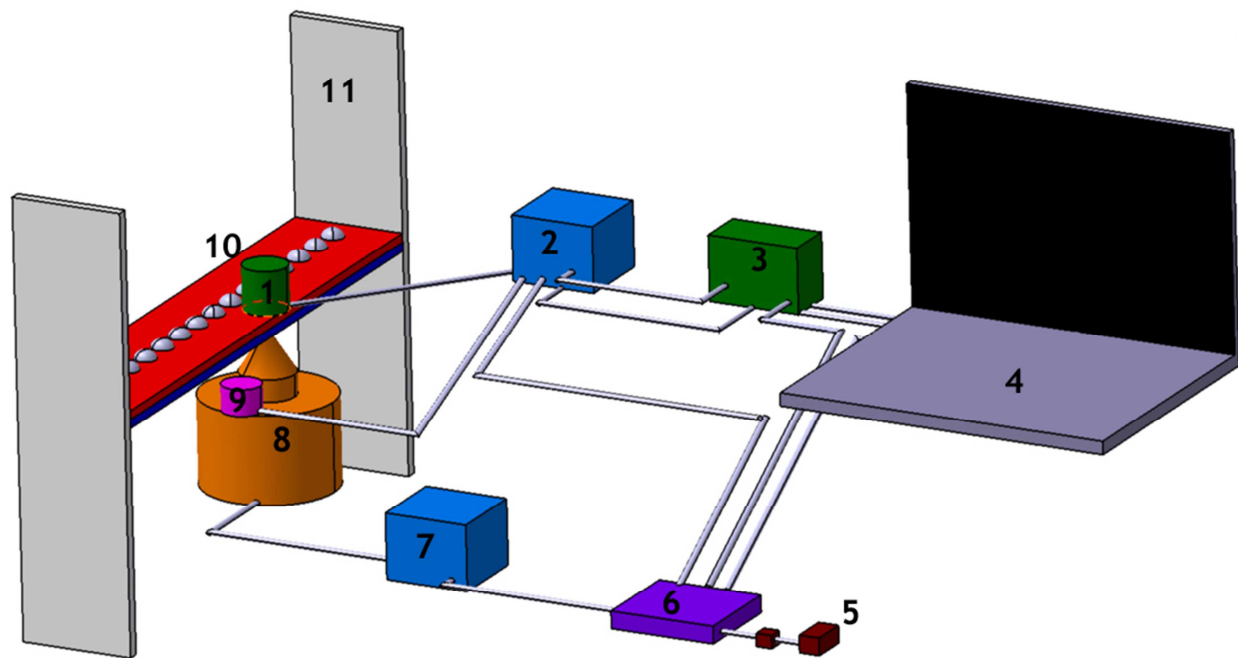


Figure 7 Schematic diagram of riveted joint in fixed-fixed beam

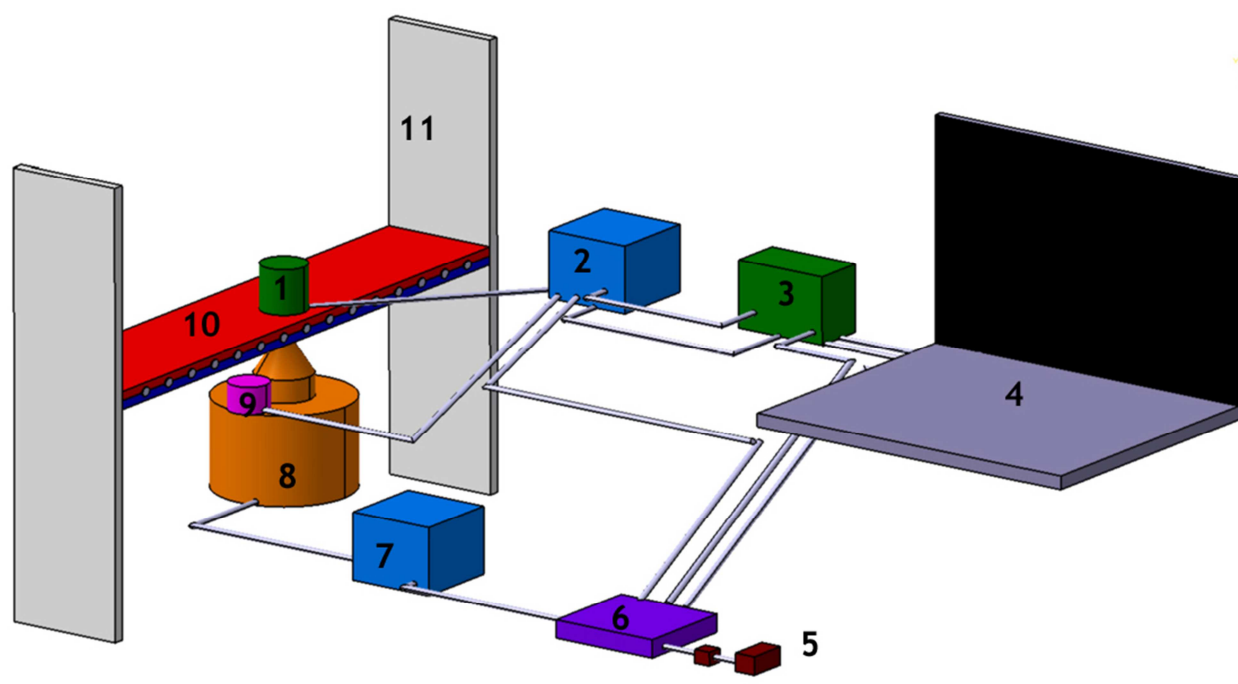


Figure 8 Schematic diagram of welded joint in fixed-fixed beam

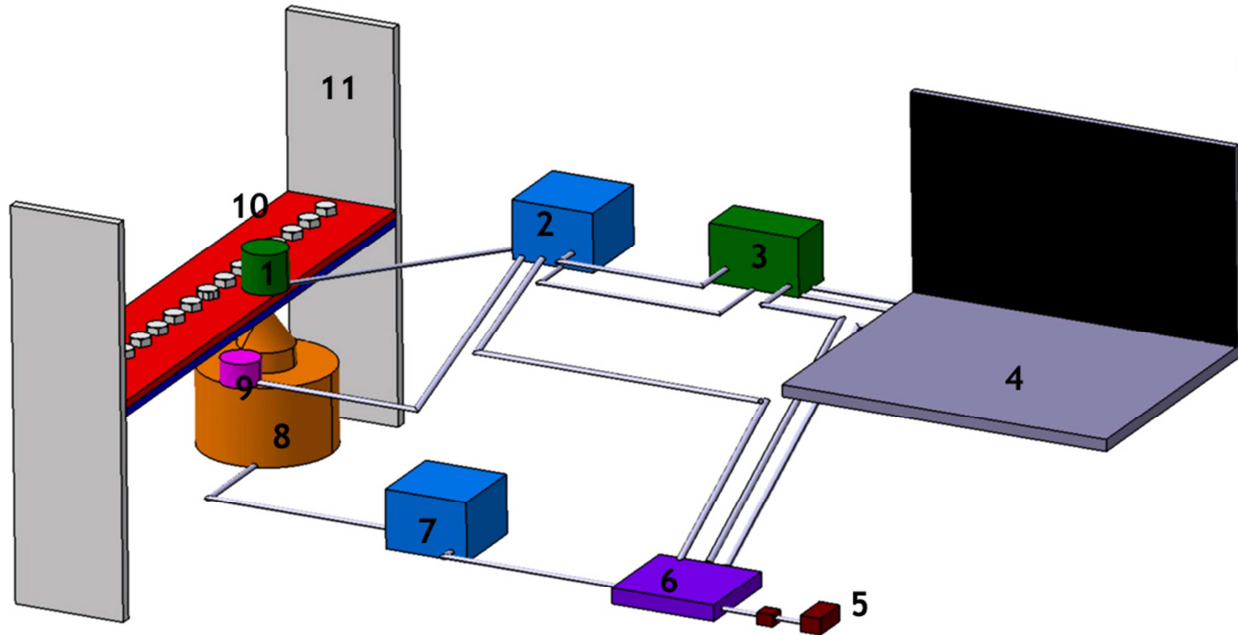


Figure 9 Schematic diagram of bolted joint in fixed-fixed beam

- | | | |
|--|------------------------|----------------------------|
| 1. Output vibration pickup | 2. Amplifier | 3. Vibration acquisition |
| 4. Vibration analyzer | 5. Power supply | 6. Distribution box |
| 7. Power amplifier | 8. Vibration generator | 9. Input excitation pickup |
| 10. Beam (riveted, welded, bolted) 11. Fixed end | | |

Table 1 Details of mild steel specimens used in the experiment for the thickness ratio 1.0 in riveted joints

Thickness X width (mm x mm)	Type of specimen	Diameter of rivet (mm)	Number of rivets used	Fixed beam length (mm)
(3 + 3) X 24.3	Jointed	12	12	291.6
(2 + 2) X 24.3	Jointed	12	10	243
(2 + 2) X 24.3	Jointed	12	9	218.7

Table 2 Details of mild steel specimens used in the experiment for the thickness ratio 1.0 in bolted joints

Thickness X width (mm x mm)	Type of specimen	Diameter of bolt (mm)	Number of bolts used	Fixed beam length (mm)
(3 + 3) X 24.3	Jointed	12	12	291.6
(2 + 2) X 24.3	Jointed	12	10	243
(2 + 2) X 24.3	Jointed	12	9	218.7

Table 3 Details of mild steel specimens used in the experiment for the thickness ratio 1.0 in welded joints

Thickness X width (mm x mm)	Type of specimen	Tack length (mm)	Number of tacks used	Fixed beam length (mm)
(3 + 3) X 24.3	Jointed	3	12	291.6
(2 + 2) X 24.3	Jointed	3	10	243
(2 + 2) X 24.3	Jointed	3	9	218.7

4.2 Instrumentation

In order to measure the logarithmic damping decrement, natural frequency of vibration of different specimen the following instruments were used as shown in circuit diagram fig:-

- (1) Power supply unit
- (2) Vibration pick-up
- (3) Load cell
- (4) Oscilloscope
- (5) Dial gauge

Load cell:

- (1) Capacity: - 5 tones

- (2) Safe Over load: - 150 % of rated capacity
- (3) Maximum Overload:- 200 % of rated capacity
- (4) Fatigue rating: - 105 full cycles
- (5) Non-linearity:- $\pm 1\%$ of rated capacity or better
- (6) Hysteresis: - $\pm 0.5\%$ of rated capacity or better
- (7) Repeatability: - $\pm 0.5\%$ of rated capacity or better
- (8) Creep error: - $\pm 1\%$ of rated capacity or better
- (9) Excitation: - 5 volts D.C. 46
- (10) Terminal Resistance:- 350Ω (nominal)
- (11) Electrical connection: - Two meters of six core shielded cable/connected
- (12) Temperature: - $\pm 10^\circ\text{C}$ to 50°C

Environmental:-

- (1) Safe operating temperature: - $+10^\circ\text{C}$ to $+50^\circ\text{C}$
- (2) Temperature range for which specimen hold good: - $+20^\circ\text{C}$ to $+30^\circ\text{C}$

Oscilloscope: -

Display: - 8x10 cm. rectangular mono-accelerator c.r.o. at 2KV e.h.t.

Vertical Deflection: - Four identical input channels ch1, ch2, ch3, ch4.

Band-width: - (-3 db) D.C. to 20 MHz (2 Hz to 20 MHz on A.C.)

Sensitivity: - 2 mV/cm to 10 V/cm in 1-2-5 sequence.

Accuracy: - $\pm 3\%$

Variable Sensitivity :-> 2.5 % 1 range allows continuous adjustment of sensitivity from 2mV/cm to V/cm.

Input impedance: - 1M/28 PF 47

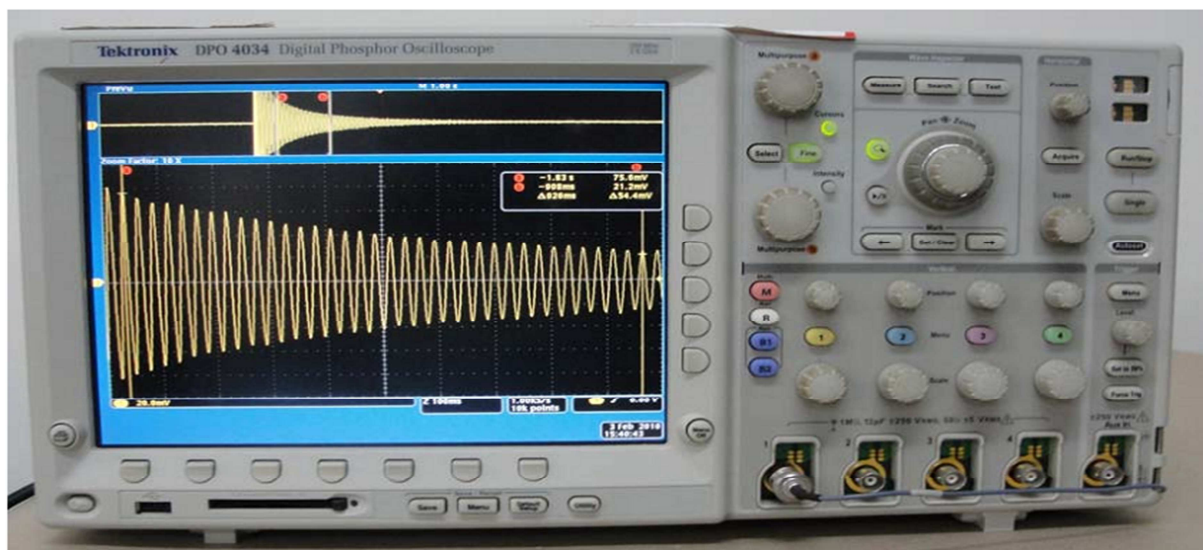


Figure 10 storage oscilloscope

An oscilloscope measures two things:

- Amplitude in time domain
- Amplitude in frequency domain

An electron beam is swept across a phosphorescent screen horizontally (X direction) at a known rate (perhaps one sweep per millisecond). An input signal is used to change the position of the beam in the Y direction. The trace left behind can be used to measure the voltage of the input signal (off the Y axis) and the duration or frequency can be read off the X axis. An oscilloscope

is a instrument which admit you to look at the shape of electrical signals by arranging a graph of voltage versus time on its screen. Gratitude with a 1cm grid enables you to calculate measurements of voltage and time after the screen. The graph is the clear and is drawn by a beam of electrons knock the phosphor coating of the screen and making it to emit, usually green or blue. This resembles the way a television picture is produced. Oscilloscopes contain a vacuum tube with a (negative electrode) at one end to emit electrons and an (positive electrode) to fasten them so they move quickly down the tube to the screen. This compact is called an electron gun. The tube also contains electrodes to avoid the electron beam up and down and left and right. The electrons are termed cathode rays because they are released by the cathode and this provides the oscilloscope its full term of cathode ray oscilloscope or CRO.

A dual dash oscilloscope can spectacle two traces on the screen, allowing you to easily analyze the input and output of an amplifier. For example, It is well virtue paying the modest extra cost to have this ability.

4.3 Connecting an oscilloscope

The Y INPUT lead to an oscilloscope should be a co-axial lead and the diagram shows its agreement. The central wire transmits the signal and the screen is compared to earth (0V) to shield the signal from electrical hindrance (usually called noise). Oscilloscopes require a BNC Socket for the y input and the main is connected with a push and braid action to uncouples you need to braid and pull.

An oscilloscope is connected like a voltmeter but you must be alert that the screen (black) connection of the input lead is compared to earth at the oscilloscope! This means it need to be connected to earth or 0V on the circuit presence is tested. Obtaining a fine and stable trace

Once you have affixed the oscilloscope to the circuit you desire to test you will need to adapt the controls to obtain a clean and stable evident on the screen.

These are discerning on more-sophisticated analog oscilloscopes, which comprise a second set of timebase circuits for a delayed sweep. A delayed sweep provides an in detail look at some small selected chunk of the main time base. The main timebase assists as a controllable delay, after which the overdue timebase starts. This can start when the delay finishes, or can be triggered (only) after the delay lapses. Ordinarily, the delayed timebase is set for a earlier sweep, sometimes much faster, such as 1000:1. At acute ratios, jitter in the delays on continuous main sweeps demeans the display, but delayed-sweep triggers can over whelm that. The display shows the vertical signal in one of numerous modes—the main timebase, or the delayed timebase only, or a mixture. When the delayed sweep is active, the main ambit trace shines while the delayed sweep is advancing. In one grouping mode, provided single on some oscilloscopes, the trace vagaries from the main sweep to the hindered sweep once the delayed sweep starts, while less of the delayed firm sweep is visible for longer delays. Another dual mode multiplexes (alternates) the main and delayed arches so that both appear at once; a trace separation control move them.

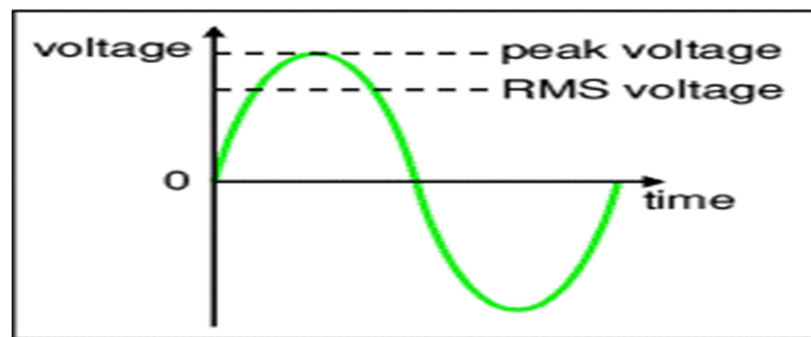


Figure 11 nodes showing voltage vs time

4.4 Voltage

Voltage is shown on the vertical y-axis and the scale is concluded by the Y AMPLIFIER (VOLTS/CM) control. Usually peak-peak voltage is measured because it can read correctly even if the reference of 0V is not known. The amplitude is partial the peak-peak voltage. To read the amplitude voltage directly you must inspect the position of 0V (normally halfway up the screen): move the AC/GND/DC switch to GND (0V) and use Y-SHIFT (up/down) to compose the position of the trace if needed, switch back to DC later you can see the signal again. Voltage = distance in cm \times volts/cm.

4.5 Time period

Time is shown on the horizontal x-axis and the scale is concluded by the TIMEBASE (TIME/CM) control. The time period (often just called period) is the time for single cycle of the signal. The frequency is the number of cycles per second, frequency = 1/time period. Ensure that the variable time base bridge is set to 1 or CAL (calibrated) before attempting to take a time reading.

4.6 Dial indicator

Dial indicator are instruments used to acutely measure a small distance. They may also be known as a dial gauge, Dial test indicator (DTI), or as a “clock”. They are named so because the measurement results are displayed in an enlarged way by means of a dial. Dial indicator may be used to check the difference in tolerance during the examination process of a machined part, measure the deflection of a beam or ring under laboratory conditions, as well as many other locations where a small measurement needs to be recorded or indicated.

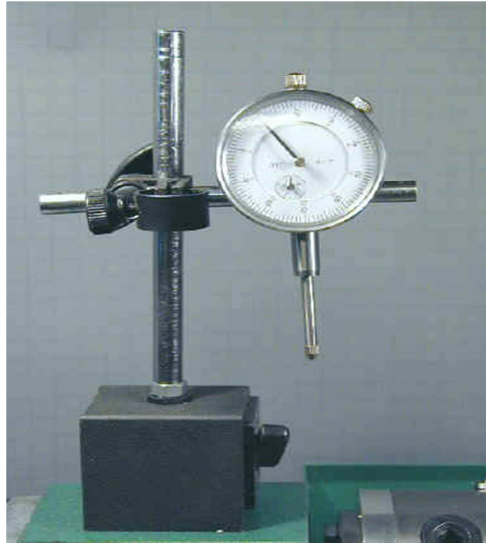


Figure 12 dial gauge

4.7 Vibration pick-up

Type: - MV-2000. Specifications:-

- (1) Dynamic frequency range: - 2 c/s to 1000 c/s
- (2) Vibration amplitude: - ± 1.5 mm max.
- (3) Coil resistance: - 1000Ω
- (4) Operating temperature: - 10°C to 40°C
- (5) Mounting: - by magnet
- (6) Dimensions: - cylindrical Length:-45 mm Diameter: - 19 mm
- (7) Weight: - 150 grams



Figure 13 vibration pickup

Velocity Transducer

The velocity pickup is a very familiar transducer or sensor for well observing the vibration of rotating machinery. This type of vibration transducer launches easily on machines, and generally costs less than other sensors. For these two explanations, this type of transducer is suitable for general drive machine applications. Velocity pickups have been used as vibration transducers on spinning machines for a very separating time, and they are quiet employed for a variety of utilizations today. Velocity pickups are amicable in many various physical configurations and output sensitivities.

4.8 Theory of Operation

When a coil of wire is stir through a magnetic field, a voltage is fortified across the end wires of the coil. The induced voltage is caused by the transferring of energy from the flux field of the Magnet to the wire coil. As the coil is accused through the magnetic field by vibratory motion, a voltage signal portray the vibration is produced.

4.8.1 Signal Conventions

A velocity signal formed by vibratory motion is commonly sinusoidal in nature. In other words, in one cycle of vibration, the signal dashes a maximum value twice in one cycle. The second maximum value is identical in magnitude to the first maximum value, but opposite in direction. By its definition velocity can be measured in only one direction. Therefore, velocity measurements are typically observed in zero to peak, RMS units. RMS units may be detailed on permanent display installations to do correlation with evidence together from small data collectors.

Another convention to consider is that motion towards the ground of a velocity transducer will access a positive going output signal. In other words, if the transducer is held in its sensitive axis and the base is tapped, the output signal will go positive when it is gruesomely tapped.

4.8.2 Construction

The velocity pickup is a self-generating sensor desires no external devices to produce a vibration signal. This type of sensor is made of three components: a perennial magnet, a coil of wire, and spring base for the coil of wire. The pickup is filled with an oil to dampen the spring action. Due to gravity forces, velocity transducers are manufactured in a different way for horizontal or vertical axis standing. With this in mind, the velocity sensor will have a sensitive axis that must be considered when smearing these sensors to twirling machinery. Velocity sensors are also prone to cross axis vibration, which if great enough may damage a velocity sensor.

Wire is wound onto a hollow spindle to form the wire coil. Sometimes, the wire coil is counter wound (wound one direction and then in the opposite direction) to counteract external electrical

fields. The spindle is supported by thin, flat coils to position it precisely in the stable magnet's field.

4.9 Experimental Techniques

In order to analyze the numerical results enumerated by the theory with the actual logarithmic damping decrement of structural jointed beams, a series of experiments were conducted. The experimental set-up for fixed-fixed beams with analyzed instrumentation is shown. All specimens were tested for their natural frequency, amplitudes and logarithmic damping decrement. A load cell was located on the ground and above it.

A fastening was given on which the specimen is kept. Above the plate a screwed spindle is escalated by rotating the screw clockwise, load is initiated on the specimen as well as load cell. A certain load as per experiment is applied at the fixed end of each of the specimens. The free end and midpoint of fixed-fixed beams, respectively of the specimens was accelerated with a spring. The excitation amplitude given to the specimen is indicated in the dial gauge. Vibration signal was picked up with the help of vibration pick-up and it was fed to oscilloscope. From there it is fed to oscilloscope where amplitude and frequency of the test signal were measured. From this logarithmic damping decrement and frequency of vibration were calculated. The specimens were prepared from commercial mild steel strips by joining layers using various joints. The lengths of the specimens were assorted, the specimens are rigidly fixed to the support to obtain perfect end conditions and the first experiments were conducted to determine the bending modulus of elasticity (E) of the specimen materials. Solid specimens made from the same set of commercial mild steel bands were held rigidly at the fixed end and their deflection (\ddot{A}) was measured by applying variety of static loads W . From these static loads and the

corresponding deflections, the average static bending stiffness (W/Δ) was determined. The bending modulus for the specimen material was then evaluated using the equation

$$E = \left(\frac{W}{\Delta} \right) \left(\frac{l^3}{3I} \right).$$

The static bending stiffness (k) of the jointed specimens was actuated and found

to be always lower than that of an equivalent solid specimen. The logarithmic damping decrement and natural frequency of vibration of all the specimens were determined experimentally at their first mode of free vibration. The lengths of these specimens were also assorted during experimentation. A spring loaded exciter was used to excite the specimens. Tests were conducted using various amplitudes of excitation (0.1, 0.2, 0.3, 0.4, 0.5 mm.) for all the specimens tested under the different conditions. The free vibration was sensed with a magnet based vibration pick-up and the corresponding signal was handed to a storage oscilloscope to obtain a steady signal. The logarithmic damping decrement was then evaluated from the measured values of the amplitudes of the first cycle (a_1), last cycle (a_{n+1}) and the number of cycles (n) of the steady signal by using the equation $\delta = \frac{1}{n} \ln \left(\frac{a_1}{a_{n+1}} \right)$. The corresponding natural frequency and time period for the first mode of vibration of the layered and jointed beam is directly recorded from the storage oscilloscope.

CHAPTER – 5

RESULTS AND DISCUSSION

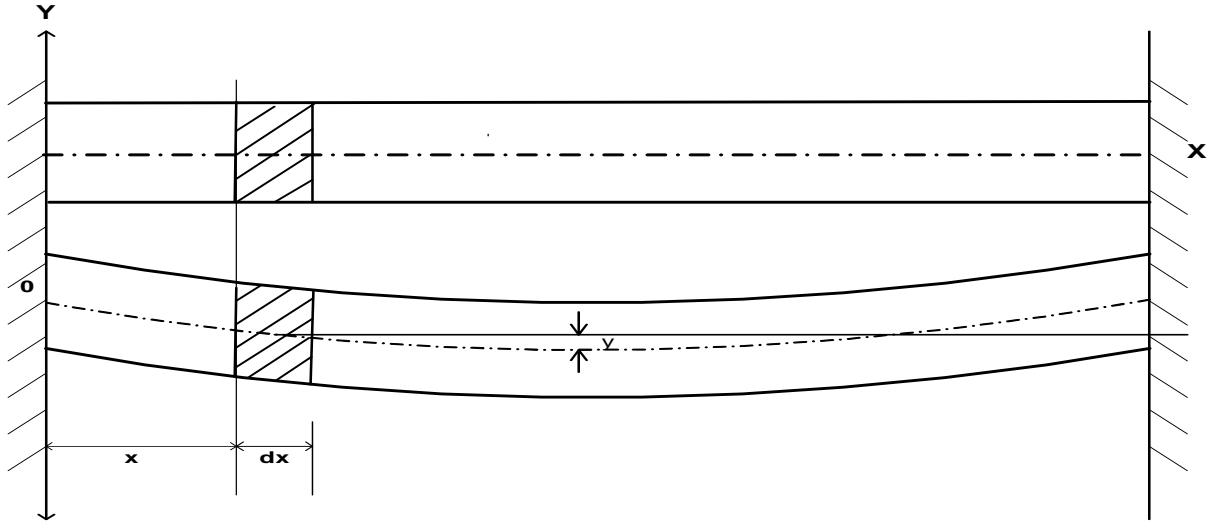


Figure 14 deflection for fixed-fixed beam

By changing the pressure, width and thickness we can find the values of the influencing parameters theoretically using matlab software.

5.1 Results for coefficient of friction $\mu * \alpha$ versus frequency

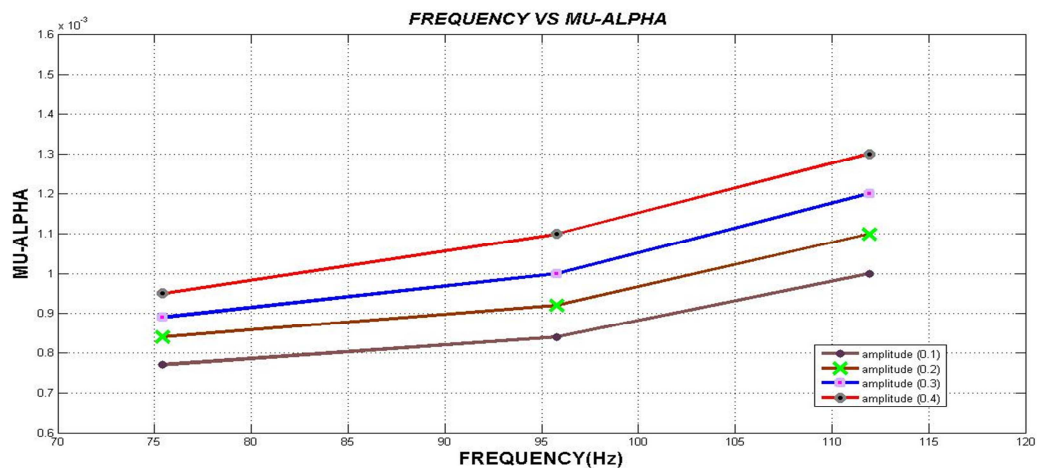


Figure 15 Variation of $\alpha.\mu$ with frequency of vibration for mild steel specimens for fixed beam in rivet joint

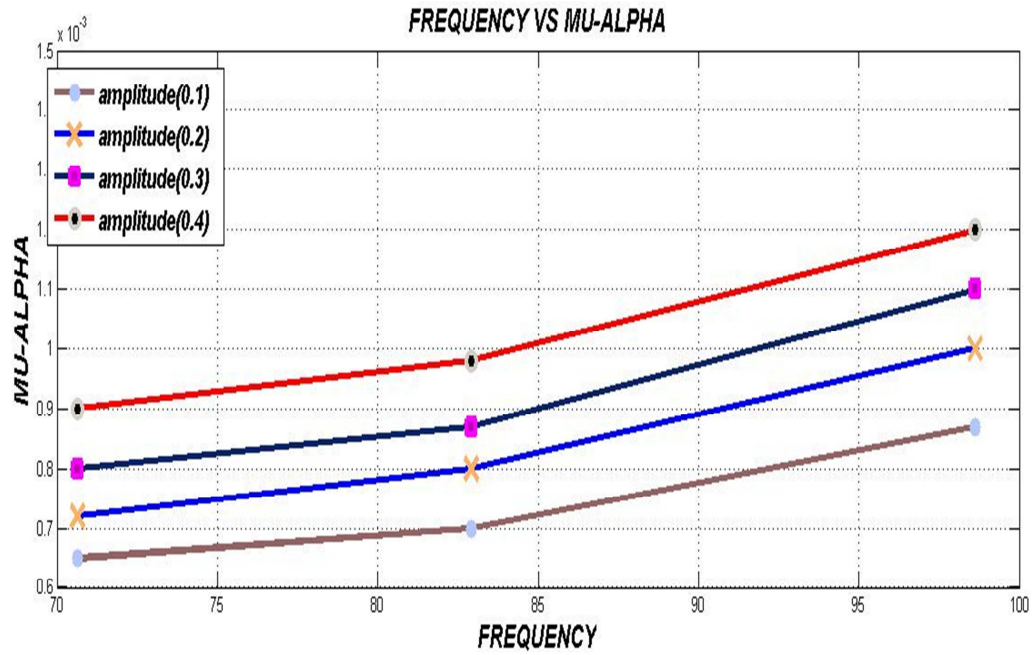


Figure 16 Variation of $\alpha.\mu$ with frequency of vibration for mild steel specimen for fixed beam in bolted joint

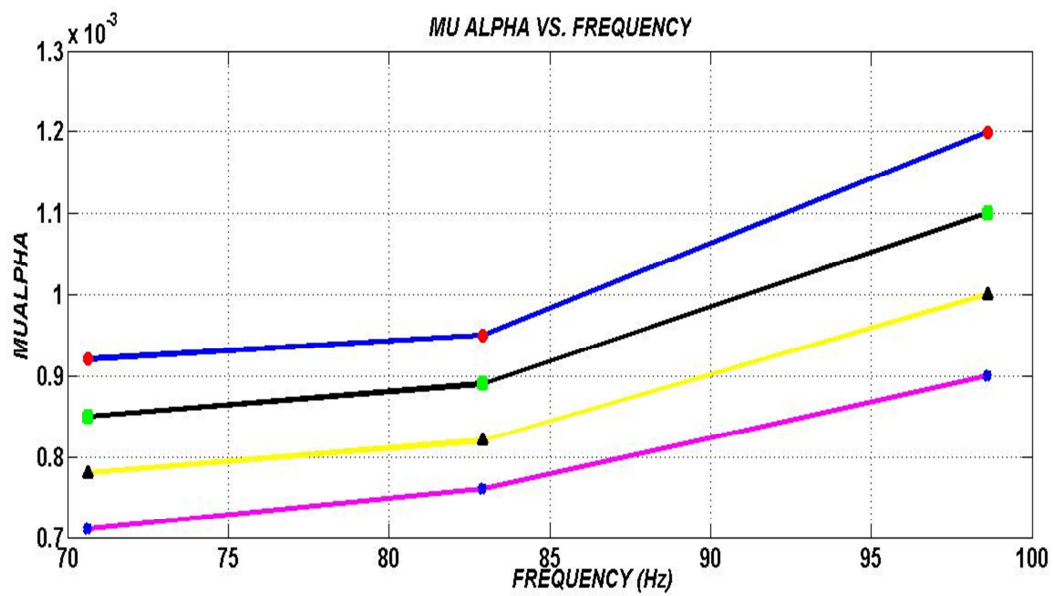


Figure 17 Variation of $\alpha.\mu$ with frequency of vibration for mild steel specimen for fixed beam in welded joint

5.2 Results for variation of logarithmic decrement with length of specimen for fixed-fixed beams

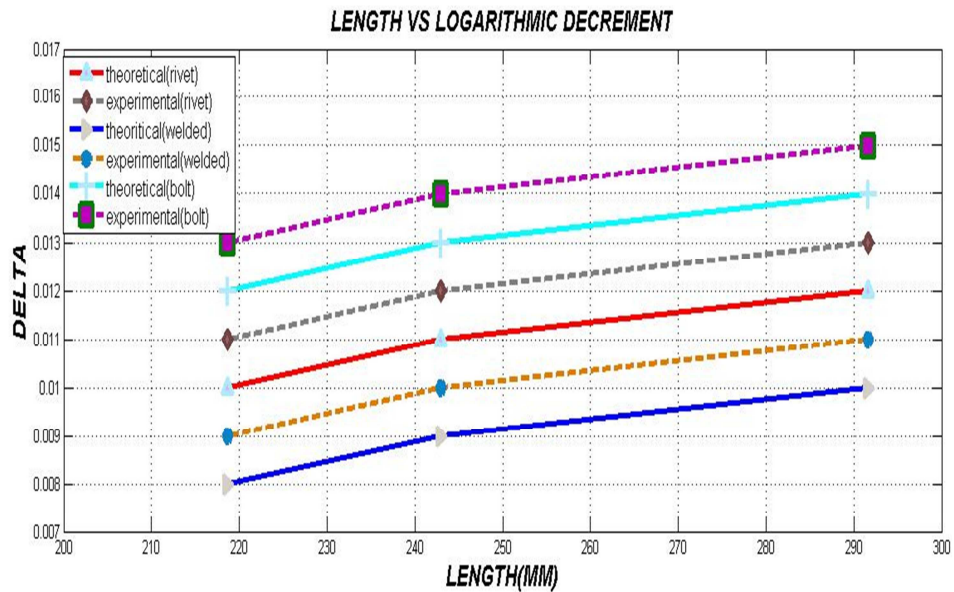


Figure 18 Variation of logarithmic decrement with the length of specimen of mild steel with amplitude of excitation 0.1 mm.

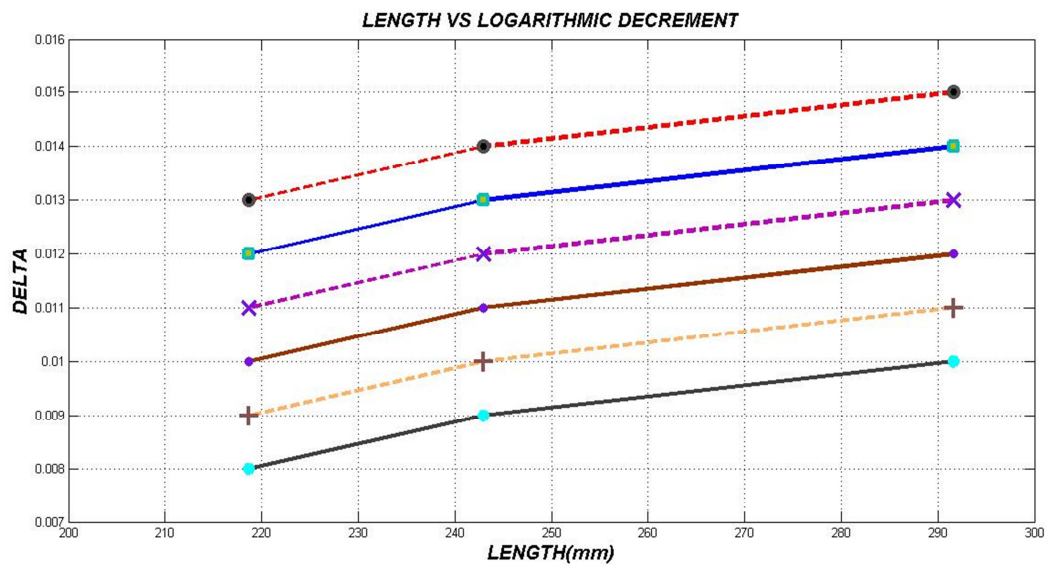


Figure 19 Variation of logarithmic decrement with the length using mild steel with amplitude of excitation 0.3 mm.

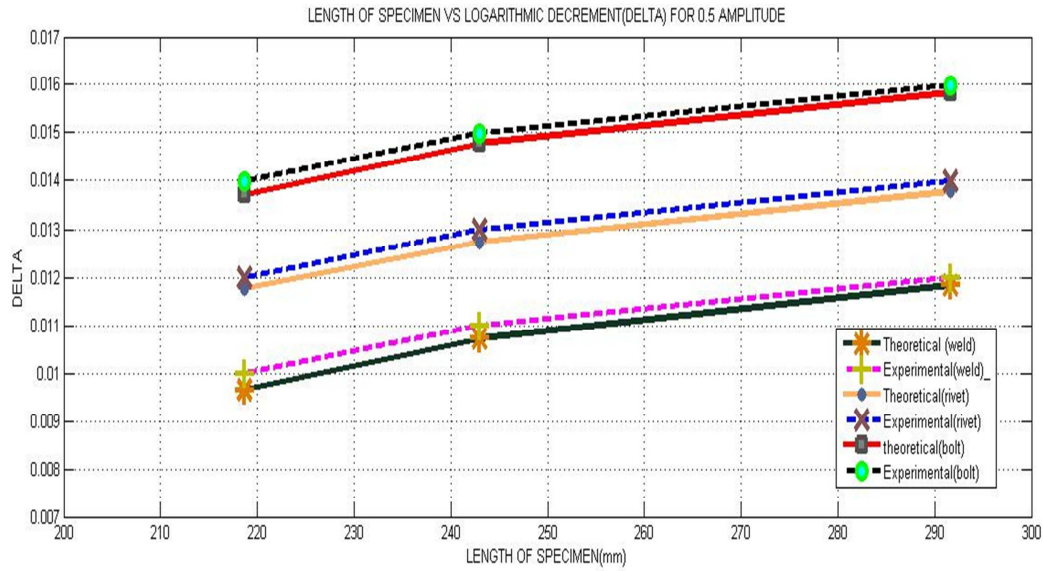


Figure 20 Variation of logarithmic decrement with the length using mild steel with amplitude of excitation 0.5 mm.

5.3 Result for variation of logarithmic decrement with amplitude of excitation for fixed-fixed beam by varying length

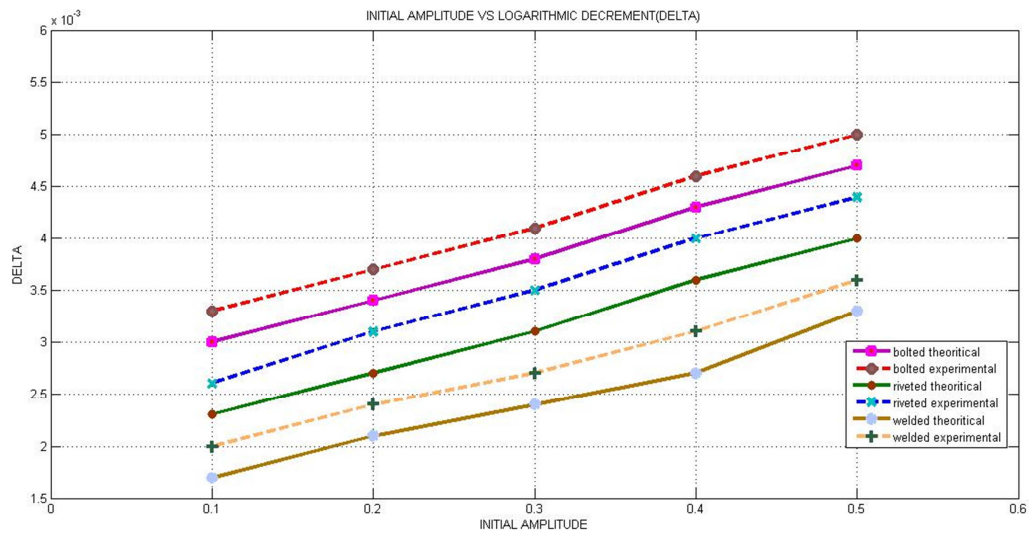


Figure 21 Variation of logarithmic decrement with initial amplitude of excitation

5.4 Result for variation of logarithmic decrement with torque for fixed-fixed beam:

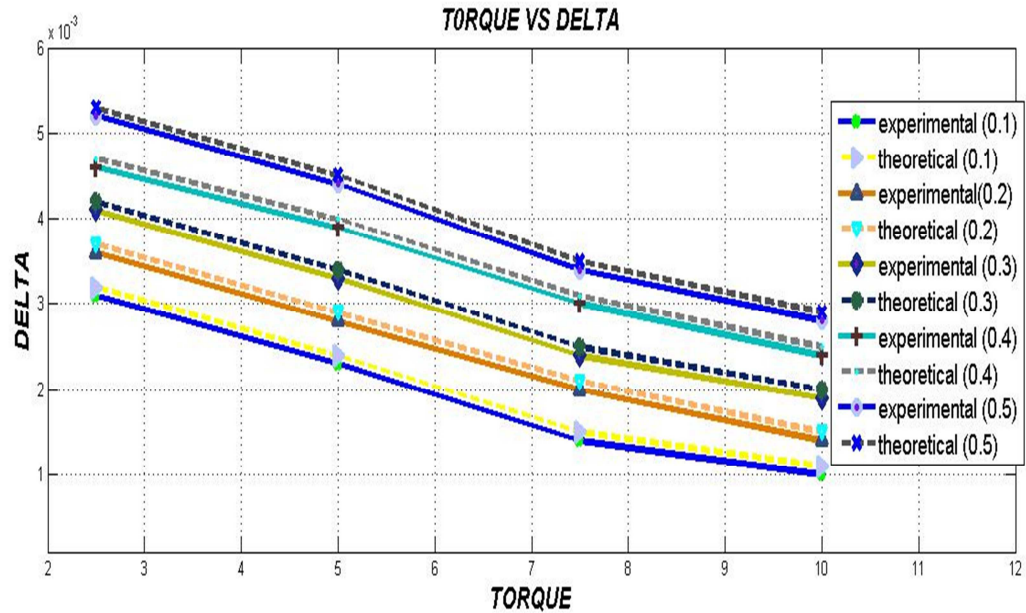


Figure 22 Variation of logarithmic decrement with applied tightening torque

5.5 Result for variation of logarithmic decrement with diameter of rivet and bolt joints

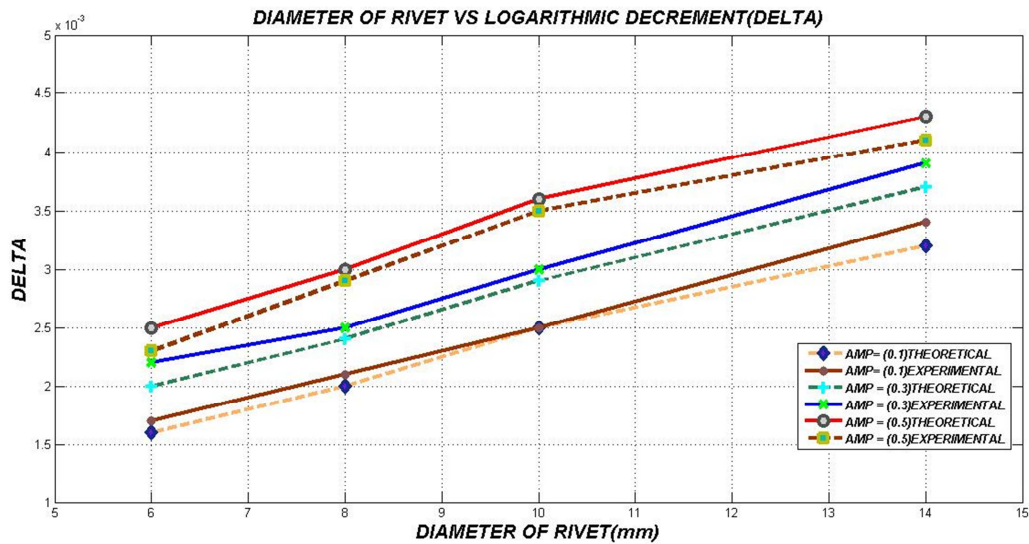


Figure 23 Variation of logarithmic decrement with diameter of rivet of 1.0 thickness ratio

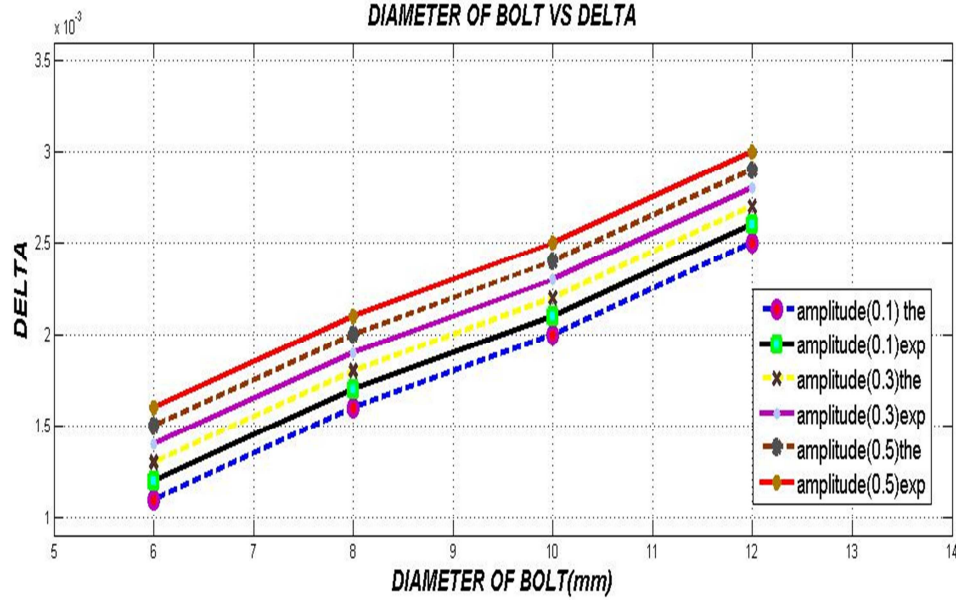


Figure 24 Variation of logarithmic decrement with diameter of bolt of 1.0 thickness ratio

DISCUSSION

- (1) Damping ratio of jointed structures declines by increase in the initial amplitude of excitation. Through an increase in initial amplitude of excitation the input strain energy bowed on the structure is increased.
- (2) Damping ratio of jointed structures increases with a rise in the length. The increase in length results in an enlarged interface length thereby resulting in an amplified area for energy dissipation of the structures. Thus increased contact area results in more energy dissipation.
- (3) Damping ratio increases by increase in diameter. The increase in initial amplitude results that there is an increase in logarithmic decrement with diameter of rivet and bolt.
- (4) The interface pressure distribution and relative space of the successive connecting bolts rivets and tacks are found to play major roles on the damping capacity of the structures.

CHAPTER – 6

*CONCLUSIONS AND
SCOPE FOR FURTHER
WORK*

Conclusions

Automated joints and fasteners are primary sources of improving damping in structural design caused by friction and micro-slip between the interfaces. The damping of jointed structures has been studied hypothetically considering the energy loss due to friction and the dynamic slip. Further, the theoretical results gained by using mathematical models like Euler-Bernoulli's theory of continuous model approach have been verified by showing widespread experiments for the validation of results.

From the prior discussions, it is found that the damping of bolted, welded and riveted structures can be amended by the following influencing parameters: (a) amplitude of excitation, (b) frequency of excitation, (c) length of specimens (d) end condition of the beam specimen (e) tightening of torque for bolted (f) pressure distribution.

The damping capacity of fixed-fixed beams of thickness ratio 1 with riveted, bolted, and welded joints has been evaluated theoretically using the energy approach.

- The interface pressure distribution and relative spacing of the consecutive connecting bolts and rivets are found to play major roles on the damping capacity of the structures.
- There is a decrease in the static bending stiffness with an increase in the length of the specimen so that the strain energy presented into the system is declined. There is an increase in the amplitude of vibration results in more input strain energy to the system.

- The damping capacity increases with increase in amplitude of excitation and length of the fixed-fixed beam whereas the same decreases with increase in tightening torque and frequency of vibration.

The values obtained from theoretical and experimental values concludes that damping capacity is higher in bolted joints, moderate in riveted and least in welded joints.

These structures being largely used in bridges, pressure vessels, frames, trusses and machine members can be effectually planned to improve the damping physiognomies so as to minimize the devastating effects of vibration and thereby increasing their life.

SCOPE AND FURTHER WORK

In the current exploration, the appliance of damping and the various parameters affecting the damping capacity of jointed structures have been obtained in detail to allow the engineers to design the structures provisional upon their damping capacity in actual applications.

- The problem can be studied considering the nonlinearity effects of slip, friction and joint properties.
- The analysis can be extended to other boundary conditions such as cantilever, fixed-supported, supported-supported, etc.
- Present analysis can be extended for forced vibration conditions.
- The analysis can be made for jointed beams of dissimilar materials.
- The present analysis can be further studied by using cantilever beams.

REFERENCES

- [1] Cochardt, A.W., 1954, A method for determining the internal damping of machine members, ASME, Journal of Applied Mechanics, Vol. 76, No. 9, pp. 257-262.
- [2] Goodman, L.E. and Klumpp, J.H., 1956, Analysis of slip damping with reference to turbine-blade vibration, ASME, Journal of Applied Mechanics, Vol. 23, pp. 421–429.
- [3] Beards, C.F., 1992, Damping in structural joints, The Shock and Vibration Digest, Vol. 24, No. 7, pp. 3-7.
- [4] Ungar, E.E., 1973, The status of engineering knowledge concerning the damping of built-up structures, Journal of Sound and Vibration, Vol. 26, No. 1, pp. 141-154.
- [5] Gaul, L. and Nitsche, R., 2001, The role of friction in mechanical joints, ASME, Applied Mechanics Reviews, Vol. 54, No. 2, pp. 93-106.
- [6] Hartwigsen, C.J., Song, Y., Mcfarland, D.M., Bergman, L.A. and Vakakis, A.F., 2004, Experimental study of non-linear effects in a typical shear lap joint configuration, Journal of Sound and Vibration, Vol. 277, No. 1-2, pp. 327-35.
- [7] Pratt, J.D. and Pardoen, G., 2002, Numerical modeling of bolted lap joint behavior, Journal of Aerospace Engineering, Vol. 15, No. 1, pp. 20-31.
- [8] Beards, C.F. and Imam, I.M.A., 1978, The damping of plate vibration by interfacial slip between layers, International Journal of Machine Tool Design and Research, Vol. 18, No. 3, pp. 131-137.
- [9] Beards, C.F. and Williams, J.L., 1977, The damping of structural vibration by rotational slip in joints, Journal of Sound and Vibration, Vol. 53, No. 3, pp. 333-340.
- [10] Beards, C.F. 1975, Some effects of interface preparation on frictional damping in joints, International Journal Machine Tool Design and Research, Vol. 15, No. 1, pp. 77-83.
- [11] Menq, C.-H., Bielak, J. and Griffin, J.H., 1986, The influence of microslip on vibratory response, Part I: A new microslip model, Journal of Sound and Vibration, Vol. 107, No. 2, pp. 279-293.
- [12] Menq, C.H., Griffin, J.H. and Bielak J., 1986, The influence of microslip on vibratory response, Part II: A comparison with experimental results, Journal of Sound and Vibration, Vol. 107, No. 2, pp. 295-307.
- [13] Hansen, S.W. and Spies, R.D., 1997, Structural damping in laminated beams due to interfacial slip, Journal of Sound and Vibration, Vol. 204, No. 2, pp. 183-202.

- [14] Masuko, M., Ito, Y. and Yoshida, K., 1973, Theoretical analysis for a damping ratio of a jointed cantibeam, Bulletin of JSME, Vol. 16, No. 99, pp. 1421-1432.
- [15] Nishiwaki, N., Masuko, M., Ito, Y. and Okumura, I., 1978, A study on damping capacity of a jointed cantilever beam, 1st Report: Experimental results, Bulletin of JSME, Vol. 21, No. 153, pp. 524-531.
- [16] Nishiwaki, N., Masuko, M., Ito, Y. and Okumura, I., 1980, A study on damping capacity of a jointed cantilever beam, 2nd Report: Comparison between theoretical and experimental values, Bulletin of JSME, Vol. 23, No. 177, pp. 469-475.
- [17] Olofsson, U. and Hagman, L., 1997, A model for micro-slip between flat surfaces based on deformation of ellipsoidal elastic bodies, Tribology International, Vol. 30, No. 8, pp. 599-603.
- [18] Thomson, W.T., 1993, Theory of Vibration with Applications, 2nd Edition, George Allen and Unwin, London.
- [19] Den Hartog, J.P., 1931, Forced vibrations with combined coulomb and viscous friction, Transactions of the ASME, Vol. 53, No. 9, pp. 107-115.
- [20] Gaul, L. and Nitsche, R., 2000, Friction control for vibration suppression, Mechanical Systems and Signal Processing, Vol. 14, No. 2, pp. 139-150.
- [21] Clarence W. de Silva, 2000, Vibration: Fundamentals and Practice, CRC Press LLC, Boca Raton.
- [22] Sidorov, O.T., 1983, Change of the damping of vibrations in the course of operation in dependence on the parameters of bolted joints, Strength of Materials, Vol. 14, pp. 671–674.
- [23] El-Zahry, R.M., 1985, Investigation of the vibration behavior of pre-loaded bolted joints, Dirasat-Engineering Technology, Vol. 12, pp. 201–223.
- [24] Marshall, M.B., Lewis, R. and Dwyer-Joyce, R.S., 2006, Characterization of contact pressure distribution in bolted joints, Strain, Vol. 42, No. 1, pp. 31-43.
- [25] Kaboyashi, T. and Matsubayashi, T., 1986, Consideration on the improvement of the stiffness of bolted joints in machine tools, Bulletin of JSME, Vol. 29, pp. 3934–3937.
- [26] Tsai, J.S. and Chou, Y.F., 1988, Modelling of dynamic characteristics of two-bolted joints, Journal of Chinese Institute of Engineering, Vol. 11, pp. 235–245.

- [27] Shin, Y.S., Iverson, J.C. and Kim, K.S., 1991, Experimental studies on damping characteristics of bolted joints for plates and shells, ASME, Journal of Pressure Vessel Technology, Vol. 113, No. 3, pp. 402–408.
- [28] Gould, H.H. and Mikic, B.B., 1972, Areas of contact and pressure distribution in bolted joints, ASME, Journal of Engineering for Industry, Vol. 94, No. 3, pp. 864–870.
- [29] Ziada, H.H. and Abd, A.K., 1980, Load pressure distribution and contact areas in bolted joints, Institute of Engineers (India), Vol. 61, pp. 93–100.
- [30] Nanda, B.K. and Behera, A.K., 1999, Study of damping in layered and jointed structures with uniform pressure distribution at the interfaces, Journal of Sound and Vibration, Vol. 226, No. 4, pp.607-624.
- [31] Goodman, L.E. and Klumpp, J.H. Analysis of Slip Damping With Reference to Turbine Blade Vibration. Journal of Applied Mechanics, 1956, 23, 421.
- [32] Cockerham, C. and Symmons, G.R. Stability criterion for stick-slip motion using a discontinuous dynamic friction model. Wear, 1976, 40, 113–120.
- [33] Hess, D.P. et al. Normal vibrations and friction at a Hertzian contact under random excitation: theory and experiment. Journal of Sound and Vibration, 1992, 153 (3), 491–508.
- [34] Guyan, A. et al. Dynamic with Friction, Modeling, Analysis and experiment, Series on Stability, Vibration and Control of Systems. World Scientific, Singapore, 1996.
- [35] Barnett, D.M. et al. Slip wave along the interface between two anisotropic elastic half-space in sliding contact. Proceedings of the Royal Society of London, Series A, 1988, 415, 389–419.
- [36] Maugin, G.A. et al. Interfacial waves in the presence of areas of slip, Geophysical Journal International, 1994, 118, 305–316.
- [37] Goodman, L.E. A Review of Progress in Analysis of Interfacial Slip Damping, Structural Damping. J. Ruzika, Ed. (ASME), New York, 1959.
- [38] Earles, S.W.E. Theoretical Estimation of the Frictional Energy Dissipation in a Simple Lap Joint. Journal of Mechanical Engineering Sciences, 1966, 8, 207.
- [39] Murty, A.S. R. On damping of thin cantilevers, Ph.D. Thesis, Department of Mechanical Engineering, I. I. T., Kharagpur, 1971.

- [40] Masuko, M., Ito, Y., and Yoshida, K. Theoretical analysis for a damping ratio of jointed cantilever beam. *Bulletin of JSME*, 1973, 16, 1421-143.
- [41] Nishiwaki, N., Masuko, M., Ito, Y., and Okumura, I. A study on damping capacity of a jointed cantilever beam (1st Report; Experimental Results). *Bulletin of JSME*, 1978, 21, 524-531.
- [42] Motosh, M. Stress distribution in Joints of bolted or riveted connections. *Transactions of ASME, Journal of Engineering for Industry*, 1975.
- [43] Hansen, S. W. and Spies, R. Structural Damping in Laminated Beams Due to Interfacial Slip, *Journal of Sound and Vibration*, 1997, 204 (2), 183–202.
- [44] Nanda, B.K. and Behera, A.K. Study on Damping in Layered and Jointed Structures with Uniform Pressure Distribution at the Interfaces. *Journal of Sound and Vibration*, 1999, 226 (4), 607-624.
- [45] Ziada, H.H. and Abd, A.K. Load pressure distribution and contact areas in bolted joints. *Institution of Engineers (India)*, 1980, 61, 93-100.
- [46] Nanda, B.K. and Behera, A.K. Damping in layered and jointed structures. *International Journal of Acoustics and Vibration*, 2000, 5 (2), 89–95.
- [47] Nanda, B.K. and Behera, A.K. Improvement of damping capacity of structural members using layered construction. *Proceedings of Seventh International Congress on Sound and Vibration*, Garmisch-Partenkirchen, Germany, 2000, pp. 3059-3066.
- [48] Nanda, B.K. Study of the effect of bolt diameter and washer on damping in layered and jointed structures. *Journal of Sound and Vibration*, 2006, 290, 1290-1314.
- [49] Damisa, O., Olunloyo, V. O. S., Osheku, C. A., and Oyediran, A. A. Dynamic Analysis of Slip Damping in Clamped Layered Beams With Non-Uniform Pressure Distribution at the Interface. *Journal of Sound and Vibration*, 2008, 309, 349–374.
- [50] Berger, E.J. Friction modeling for dynamic system simulation. *Applied Mechanics Reviews*, 2002, 55 (6), 535–577
- [51] Beards, C.F. The damping of structural vibration by controlled interfacial slip in joints. *Journal of Vibration, Acoustics, Stress, and Reliability in Design*, 1983, 105, 369–372
- [52] Mayer, M. A. and Gaul, L. Segment-to-segment contact elements for modelling joint interfaces in finite element analysis. *Mechanical Systems and Signal Processing*, 2007, 21, 724–734

- [53] Gregory D. L., Smallwood, D. O., Coleman, R.G., and Nusser, M.A. Experimental studies to investigate damping in frictional shear joints. Proceedings of 70th Shock and Vibration Symposium, 1999.
- [54] Singh, B. and Nanda, B. K. Effect of welding on the slip damping of layered and jointed structures. Journal of Engineering Mechanics, ASCE, 2010, 136 (7), 928–932.